공학박사 학위논문

Nanoparticle-mediated induction of type II collagen-specific regulatory T cells for osteoarthritis treatment

골관절염 치료를 위해 제2형 콜라겐 특이적 조절 T세포를 유도하는 나노입자

2023년 2월

서울대학교 공과대학

화학생물공학부

손 희 수

Nanoparticle-mediated induction of type II collagen-specific regulatory T cells for osteoarthritis treatment

지도 교수 김 병 수

이 논문을 공학박사 학위논문으로 제출함
2023년 02월

서울대학교 대학원
화학생물공학부
손 희 수

손희수의 공학박사 학위논문을 인준함
2023년 02월

위 원 장 _____ 황 석 연 _____ (인)

부위원장 _____ 김 병 수 _____ (인)

위 원 _____ 백 승 렬 _____ (인)

위 원 _____ 한 지 숙 _____ (인)

위 원 _____ 조 미 라 _____ (인)

Abstract

Nanoparticle-mediated induction of type II collagen-specific regulatory T cells for osteoarthritis treatment

Hee Su Sohn

School of Chemical and Biological Engineering

The Graduate School

Seoul National University

Osteoarthritis (OA) is known as the most representative joint disease along with rheumatoid arthritis (RA). OA is accompanied by excessive formation of bone around the joint, joint deformation and pain. Currently, it is known that about 80 % of the world's population over the age of 55 and almost most of the population over the age of 75 show signs of OA. In the case of Korea, with rapid aging rate of the society, the number of people complaining of pain due to OA is gradually increasing. As a result, medical expenses are also increasing at a rapid pace. The

known treatments for OA include administration of anti-inflammatory drugs, non-pharmacologic therapy to improve lifestyle and eating habits, and invasive joint replacement surgery. Nonsteroidal anti-inflammatory drugs (NSAIDs) are effective in reducing pain through alleviation of inflammation, but gastrointestinal side effects may occur, and cyclooxigenase-2 (COX-2) inhibitor may cause cardiovascular side effects and gastrointestinal damage. Also, in the case of surgery, the cause of pain can be effectively removed, but there is a burden of possibility of reoperation depending on the condition of both the joint and the artificial joint.

In general, OA is known to be caused by wear of cartilage. However, recent articles revealed that immune system is involved in progression of OA. Therefore, understanding the immune modulation based on the action of immune cells in OA has become important.

Here, we describe an immune-modulating nanoparticle for OA treatment. Intradermal injection of lipid nanoparticles (LNPs) loaded with type II collagen (Col II) and rapamycin (LNP-Col II-R) into OA mice effectively induced Col II-specific anti-inflammatory regulatory T cells, significantly increased anti-inflammatory cytokine expression and reduced inflammatory immune cells and pro-inflammatory cytokine expression in the joints. Consequently, LNP-Col II-R injection inhibited chondrocyte apoptosis and cartilage matrix degradation and relieved pain, while injection of LNPs loaded with a control peptide and rapamycin did not induce these events. Adoptive transfer of CD 11c+ DCs and CD4+CD25+ T cells isolated from LNP-Col II-R-injected mice suggested that tDCs and Tregs induced by LNP-Col II-R injection were likely responsible for the

therapeutic effects.

Taken together, we confirmed that immunomodulatory nanoparticles carrying type II collagen peptide and rapamycin showed therapeutic effects on OA. In addition to OA, the nanoparticles used in this experiment can be used for other inflammatory diseases such as myocardial infarction, cerebral infarction, spinal cord injury, or for autoimmune diseases such as atopic dermatitis, rheumatoid arthritis, type I diabetes, or Crohn's disease by substituting the antigen for disease-specific antigens.

Keywords: tolerogenic lipid nanoparticles, tolerogenic dendritic cells, regulatory T cells, macrophages, immune modulation, osteoarthritis, synovitis

Student Number: 2017-20762

Table of contents

List of figures

Abbreviations

ANOVA	analysis of variance
Arg1	arginase 1
BAX	bcl2 associated x
CCK	cell counting kit
cDNA	complementary DNA
Col II	type II collagen
DAPI	4,6-diamidino-2-phenylindole
DC	dendritic cell
tDC	tolerogenic dendritic cell
DLS	dynamic light scattering
ECM	extracellular matrix
EDTA	ethylene-diamine-tetraacetic acid
ELISA	enzyme-linked immunosorbent assay
FBS	fetal bovine serum
H&E	Hematoxylin & Eosin
HPLC	high performance liquid chromatography
HRP	horseradish peroxidase
IA	intraarticular

IL	interleukin
IHC	immunohistochemistry
IFNγ	interferon gamma
LNP	lipid nanoparticle
LPS	lipopolysaccharide
MALDI-TOF	matrix-assisted laser desorption/ionization time-of-flight
MHC II	major histocompatibility complex type II
MMP13	matrix metallopeptidase 13
MSC	mesenchymal stem cell
OA	osteoarthritis
OARSI	osteoarthritis research society international
PBS	phosphate buffer saline
PEG	polyethylene glycol
PFA	paraformaldehyde
qRT-PCR	quantitative real-time polymerase chain reaction
RA	rheumatoid arthritis
SFO-FG	Safranin-O-Fast Green
TEM	transmission electron microscopy
TGFβ	transforming growth factor beta

TMB	3,3′,5,5′-tetramethylbenzidine
Th	helper T cells
TNFα	tumor necrosis factor alpha
Treg	regulatory T cell
TUNEL	terminal deoxynucleotidyl transferase dUTP nick end labeling

Chapter 1.

Research backgrounds and objective

1.1. Pathogenesis of OA

1.1.1. Heterogeneity of OA

OA is a well-known joint disease which is caused by various factors. The OA pathology is heterogeneous. It shows diverse clinical features, biochemical and genetic characteristics, and shows diverse responses to treatments. The factors that trigger and aggravate OA are divided into genetic, hormone- or age-related primary or intrinsic factors and traumatic injury-induced secondary or extrinsic factors [1, 2, 3]. Considering the heterogeneity of OA pathology, every treatment may not be effective for OA as a whole and could be specifically effective for cases that correspond to the treatment. Therefore, the treatments need to be optimized and tailored to suit the individual's needs.

1.1.2. OA, a low-grade inflammatory disease

OA has been traditionally considered as a non-inflammatory disease, which is caused by wear of cartilage. However, recent evidences have indicated that inflammation plays a pivotal role in the disease progression. Compared with RA which is a chronic systemic autoimmune disease, OA shows a low grade of inflammation[4]. Not only the degree of inflammation but also the infiltrated immune cells in OA synovium differs from those in RA synovium (Figure 1.1.). Once inflammation starts to develop in OA

synovium, extracellular matrix (ECM) degrading enzymes are produced and secreted from chondrocytes. The Inflammatory cytokines are secreted from both chondrocytes and the inflammatory immune cells in synovium which are activated by the inflammatory cytokines. As inflammation sustains, chondrocytes lose the ability to maintain the homeostasis of cartilage and be more susceptible to inflammation[5]. As a result, the number of inflammatory immune cells increases in synovium as compared with that of normal healthy synovium[6]. It has been known that, diverse T cell types are involved in the OA progression (Figure 1.2.). Especially, inflammatory type 1 helper T cells (Th1 cells), type 9 helper T cells (Th9 cells), type 17 helper T cells (Th17 cells), and cytotoxic T cells showed an increased profile in peripheral blood, synovial fluid and synovial membranes. On the other hand, the profile of anti-inflammatory regulatory T cells (Tregs) decreased in OA patients' peripheral blood, synovial fluid and synovial membranes. However, the involvement of Th2 cells, Th22 cells, Tfh cells in the pathogenesis of OA is lesser known than the aforementioned T cell types, therefore, needs further investigation [6].

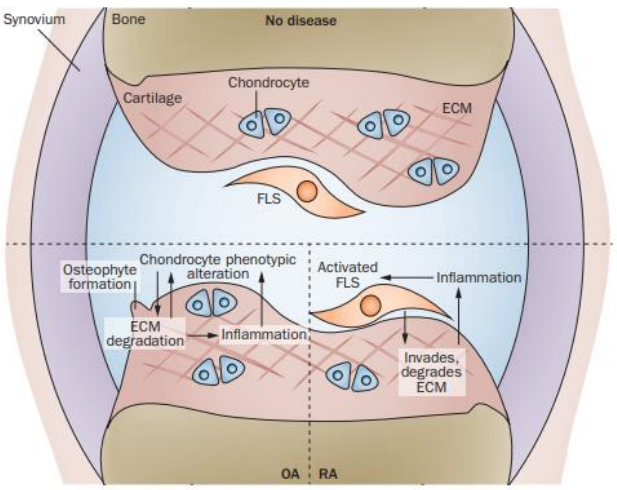

Figure 1.1. Comparison of pathology between OA and RA. The cartilage destruction of OA and RA proceeds via different pathways and mechanisms although they share some similarities [5].

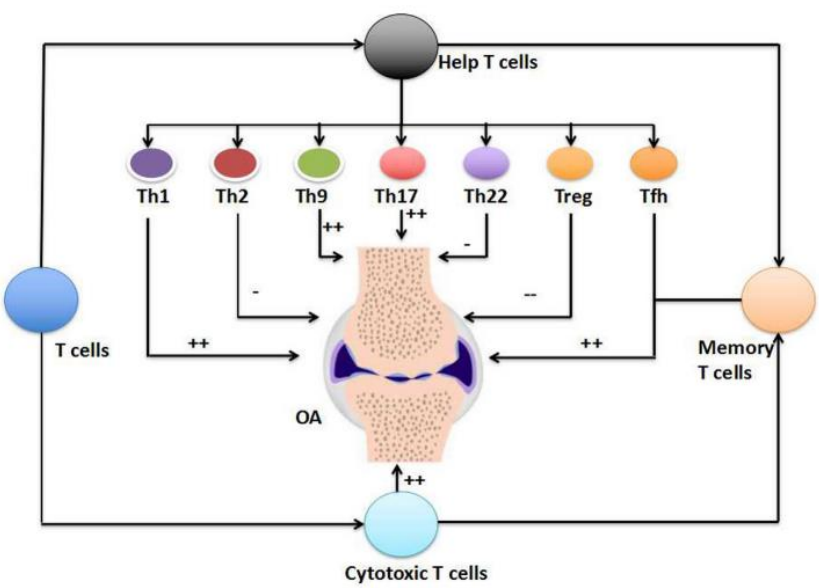

Figure 1.2. The involvement profile of T cells in pathogenesis of OA. The number of inflammatory T cells increase, while that of anti-inflammatory T cells decrease in peripheral blood, synovial fluid or synovial membranes in OA patients [6].

1.1.3. Autoantibodies in OA

Autoantibodies are found in peripheral blood and synovial fluid of OA patients, although OA is not an autoimmune disease as RA[7]. Studies have indicated that inflammation in synovium triggers the production of enzymes and chemicals that could alter proteins by citrullination, carbamylation, oxidation, and glycation. The process of post translational modification is important for increasing antigenicity and producing autoantibodies[7]. The level of antibodies against citruillinated peptides, carbamylated peptides, native or oxidised Col II in sera and synovial fluid was measured in OA and RA patients. And the result showed that autoantibodies against citrullinated and carbamylated peptides are more specifically associated with RA, while autoantibodies to collagen (anti CI/CII/ROS-CI/ROS-CII) are detected with frequencies between 15 % and 30 % in OA patients (Figure 1.3.). Furthermore, several autoantibodies against cartilage derivates were found in sera of OA patients[8]. These indicate that OA is a multi-antigenic disease and the presence of autoantibodies against type II collagen peptides verifies that type II collagen could be a possible target for OA treatment by inducing the antigen-specific immune modulation.

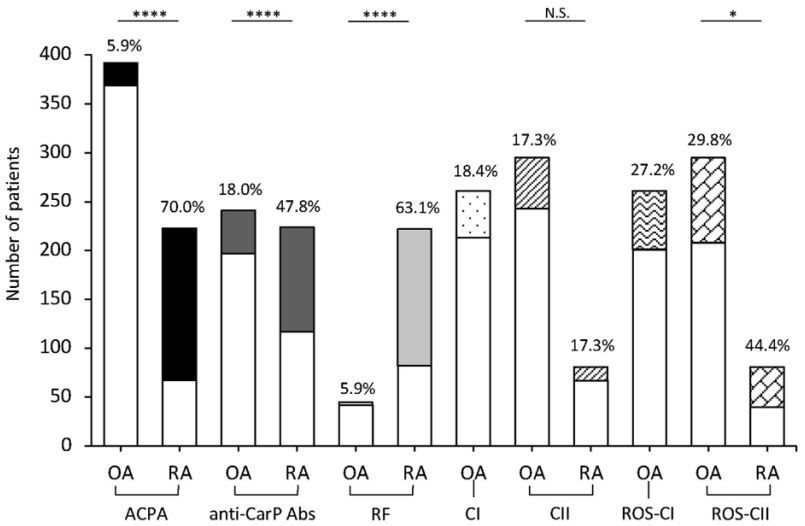

Figure. 1.3. Comparison of autoantibodies in serum of OA and RA patients. The result shows that autoantibodies against citrullinated, carbamylated peptides are more common in RA patients. In contrast, the autoantibodies against native collagen peptides and oxidized collagen peptides are detected in OA patients [7].

1.2. Conventional therapies for osteoarthritis (OA) and limitations

The general treatments for OA prior to joint replacement include oral administration of nonsteroidal anti-inflammatory drugs (NSAIDs) and injection of hyaluronic acid as well as mesenchymal stem cells (MSCs) within the joint [9]. However, these treatments relieve symptoms only to a certain extent, cannot stop the progression of the disease, and often cause side effects. The administration of NSAIDs is known to cause gastrointestinal side effects in some cases. Autologous chondrocyte implantation can be used to regenerate cartilage in OA

patients[10]. But this method requires a process of massive *ex vivo* culture of chondrocytes which is costly and invasive. Implantation of MSCs in intraarticular cavity is another effective method to alleviate the symptoms of OA. MSCs are able to differentiate into desired cell types under specific circumstances and to exert immunomodulation through paracrine mechanisms. However, implantation of MSCs also has some limitations and needs further investigation. *In vitro* culture of MSCs requires time and effort, and the engraftment efficiency at target site differs from freshly isolated cells[11]. After delivering the cells to OA joint, attachment of cell at desired site, differentiation of MSCs to desired cell types, and prolonged cell viability is not always guaranteed[11, 12]. Finally, the joint replacement is the most direct way to solve the problem by removing the inflammatory tissue from the target site surgically. This method is effective yet highly invasive.

1.3. Lipid nanoparticles (LNPs) : potential clinical agent

1.3.1. Lipid nanoparticles

Lipid nanoparticles like liposomes are nano-sized particles which are composed of lipids. The lipophilic tail and hydrophilic head of lipids allow lipid nanoparticles to have unique structures, such as hydrophilic core and hydrophobic shell. This allows lipid nanoparticles to load hydrophilic and lipophilic drugs at the same. The lipid nanoparticles are generated by the well-known thin film hydration method (Figure 1.4.)[13]. The lipids as well as hydrophobic drugs are dissolved in organic solvents. After mixing the lipid and lipophilic drug solutions, the organic solvents were removed by evaporating the solvents. The evaporating process could be preceded under rotary vacuum pump at a temperature of 45 ℃, while the organic solvent under a volume of 1 ml is dried with a dry nitrogen or argon gas in a fume hood. The generated thin lipid film is then hydrated by adding aqueous solutions containing hydrophilic drugs. Multi lamellar vesicles are generated by stirring the hydrated solutions thoroughly. Extra downsizing steps of extrusion, homogenization, or sonication are required in order to generate small unilamellar vesicles.

Lipid nanoparticles are efficient for delivering drugs to target cells or tissues by encapsulating the drugs within the structure of lipid bilayer. So far 15 drugs with liposomal delivery system are FDA approved and are available on market and more than 40 additional liposomal drugs are under clinical trials[14]. Despite the effective drug delivery, few drawbacks exist and additional structural modifications are required to overcome the problems[14].

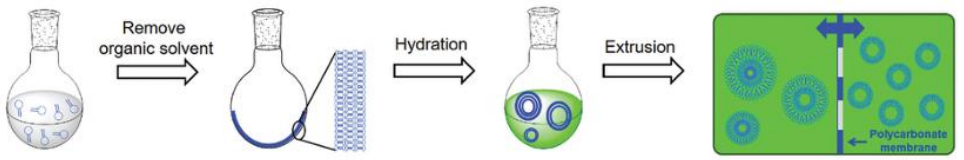

Figure 1.4. Scheme of thin film hydration method to produce lipid nanoparticles as liposomes.

1.3.2 Lipid nanoparticles as an alternative therapy for OA treatment

Lipid nanoparticle, a possible disease modifying osteoarthritis drug (DMOAD), is introduced to treat OA. There are so far no definite cures for OA, therefore, most treatments focus on relieving symptoms, pain and regaining function. The commonly used drugs for OA are inflammation inducing prostaglandin producing cyclooxygenase-2 (COX-2) inhibitors, non-steroidal anti-inflammatory drugs (NSAIDs), and corticosteroids [15]. The drugs are orally administered and they occasionally cause gastrointestinal and cardiovascular side effects due to systemic administration. Considering that inflammation occurs locally in joint tissue, local administration of drugs into intraarticular (IA) joint could be an alternative pathway to deliver drugs to OA joint[16]. Due to low permeability to chondrocytes and fast removal of drugs after IA injection, especially small molecules, alternative methods of using lipid nanoparticles are introduced to deliver drugs more effectively[16]. Various types of drugs could be loaded in lipid nanoparticles, such as lubricin, hyaluronan, anti-inflammatory molecules, or anti-oxidants. Lipid nanoparticles have advantages of increasing biocompatibility, loading and

delivering large amount of drugs at a time, and loading both hydrophilic and lipophilic drug at once. Despite these advantages, the stability of lipid nanoparticles needs to be strengthened for further usage.

1.4. Cell-nanoparticle interaction

When nanoparticles are incubated with cells, the particles first meet the plasma membrane of cells and are internalized into cells via endocytosis process [17]. Some of the endocytosed nanoparticles escape from cells via exocytosis process. Cellular responses to nanoscale-materials depend on both physicochemical properties of materials and cell types. The size and shape of nanostructures have effect on the efficiency of endocytosis and exocytosis. Furthermore, the materials rarely take up by nonphagocytic cells can be internalized into phagocytic cells. Dendritic cells (DCs) are one of the antigen presenting cells that uptake foreign particles and induce innate and subsequently adaptive immune responses by secreting soluble mediator and presenting the processed foreign peptides on major histocompatibility complex II (MHC II) (Figure 1.5.). In order to increase the uptake efficiency by DCs, modification of lipid nanoparticles is necessary [18, 19]. Changing the surface charge, incorporating mannosylated lipids and conjugating specific receptor targeting antibodies to lipid nanoparticles' surface might increase the uptake of lipid nanoparticle by DCs [19].

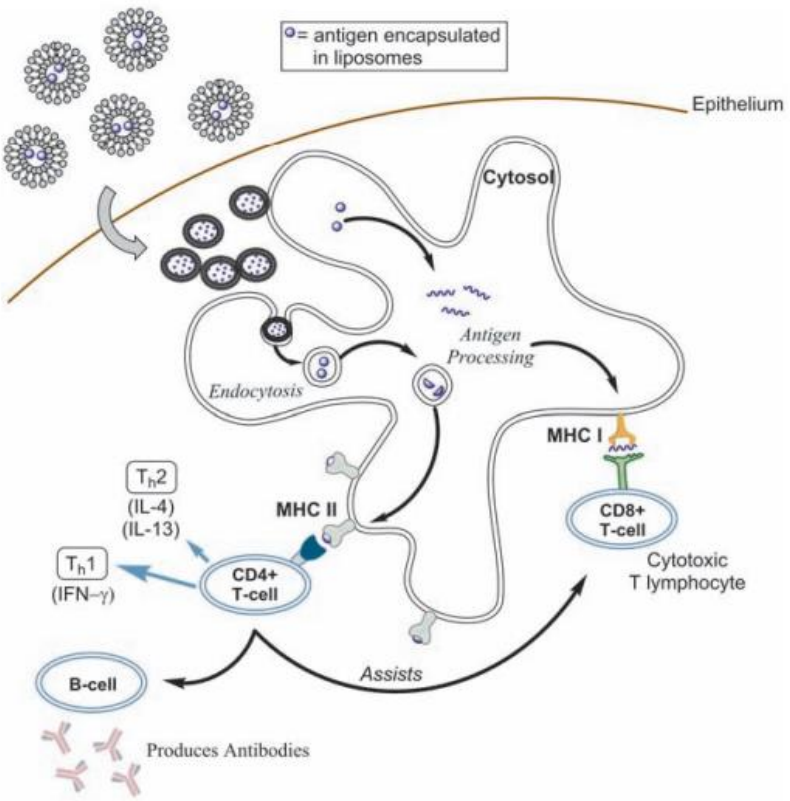

Figure 1.5. Scheme of nanoparticles as liposomes uptake by DCs[19]

1.5. Research objective of thesis

The research objective in this thesis is the enhancement of the therapeutic efficacy of tolerogenic LNPs for immunomodulatory therapy to treat inflammatory diseases, such as osteoarthritis. In this thesis, we suggest the therapeutic applications of tolerogenic LNPs loaded with type II collagen peptide and rapamycin .

The chapter 3 reports the therapeutic effects of the tolerogenic LNPs.

Applications of lipid nanoparticles for OA treatment have been studied, however, loading inflammation alleviating drugs limits the therapeutic potential of LNPs for relieving inflammation temporarily. No study has applied OA antigens to enhance the therapeutic potential of LNPs for OA treatment. We developed type II collagen peptide and rapamycin incorporated LNPs for OA treatment. The loading of type II collagen peptides not only upregulates therapeutic effects by inducing type II collagen-specific Tregs but also facilitates high retention of type II collagen-specific Tregs in the targeted joint area. The induced OA-specific Tregs can contribute to polarize macrophages from pro-inflammatory subtype to anti-inflammatory subtype, inhibit inflammatory immune cells, protect chondrocytes from apoptosis, prevent cartilage ECM degradation, and subseuquently relieve pain. *In vitro*, LNP-Col II-R showed significantly enhanced cellular uptake, antigen presentation, induction of tolerogenic dendritic cells, and antigen specific Tregs. *In vivo*, indeed, the injection of LNP-Col II-R markedly attenuated cell death, cartilage degradation, and inflammation which ultimately resulted in pain relief.

Chapter 2.

Experimental methods

2.1. Cell isolation and culture

Bone marrow-derived dendritic cells (BMDCs) were isolated from 6-week-old female C57BL/6 mice (OrientBio, Gyeonggi, South Korea). After proper trimming, the tops of both the femur and tibia were cut and placed in two Eppendorf tubes that were stacked together. The tip of the inner smaller tube was holed using an 18G needle. The tubes were spun at 13500 rpm for 1 minute. The isolated bone marrow cells were reconstituted in Roswell Park Memorial Institute (RPMI) 1640 medium containing 10% fetal bovine serum (FBS), 100 units/ml penicillin and 100 μg/ml streptomycin, 50 μM 2-mercaptoethanol (Sigma Aldrich, USA) and 20 μg recombinant murine granulocyte macrophage colony-stimulating factor (rmGM-CSF) (PeproTech, USA). The solution was filtered through a 70-μm cell-strainer. Cells were plated in a 100-mm dish at a concentration of 2 x10^5 cells/ml and cultured. After 3 days, 10 ml of fresh medium was added. DCs collected at day 10 were used for further experiments.

OVA-specific T cells were isolated from OT-II transgenic mice. 1 ml of ACK lysis buffer (Thermo Fisher Scientific, USA) was added to the harvested spleen and the organ was minced thoroughly with the thumb rest of the syringe. 9 ml of RPMI

1640 cell media was added and the splenocytes were filtered through a 70-μm cell-strainer. The cell solution was centrifuged at 1500 rpm for 5 minutes. The isolated splenocytes were reconstituted in RPMI 1640 medium and seeded in a 96 well plate for further experiments.

2.2. Preparation and characterization of materials

2.2.1. Preparation of type II collagen peptides

Col II was prepared by treating type II collagen (Chondrex, Inc., USA) with collagenase III (Stemcell Technologies, Canada). In OA development, primarily collagenase III (MMP-13) is known to degrade the cartilage matrix. Type II collagen and collagenase III (10 U/ml) were dissolved in 0.05 M acetic acid and PBS, respectively. The solutions were mixed and incubated overnight with stirring.

2.2.2. Characterization of type II collagen peptides

After collagen digestion, the molecular weight of Col II was determined by matrix-assisted laser desorption/ionization time-of flight (MALDI-TOF) mass spectrometry (Spotlight400, Perkin Elmer, USA).

2.2.3. Preparation type II collagen peptides and rapamycin incorporated lipid nanoparticles (LNP-Col II-R)

LNPs were synthesized with a conventional thin film hydration method [20]. Briefly, 1,2-dioleoyl-3-trimethylammonium-propane (chloride salt) (DOTAP), 1,2-dioleoyl-sn-glycero-e-phosphethanolamine (DOPE), and 1,2-distearoyl-sn-glycero-3-phosphoethanolamine-N-[methoxy(polyethylene glycol)-2000] (ammonium salt) (PEG2000 PE) were dissolved in chloroform. Cholesterol and rapamycin were dissolved in 100% pure ethanol. DOTAP, DOPE, cholesterol, and PEG PE were placed in glass vials at a molar ratio of 0.475: 0.35: 0.12: 0.05. Before dehydration, 70 μg of rapamycin was added. The vial was agitated at 40 °C until the solvents dried. Then, 100 μg of Col II was added to the vial. PBS

was added for hydration until the total volume became 1 ml. The hydrated solution was serially extruded through 1-μm, 400-nm and 200-nm pore size filters. The extruded nanoparticles were concentrated twice using 100K Amicon® Ultra-0.5 centrifugal filter devices (Merck Millipore, USA) at 14000 g for 30 minutes.

2.2.4. Characterization of LNP-Col II-R

The shape of LNPs was characterized with transmission electron microscopy (TEM, JEM-F200 (TFEG), JEOL Ltd, Japan). The size and zeta potential of LNPs were determined by dynamic laser scattering (DLS, Zetasizer Nano ZS, Malvern Panalytical, UK). For size analysis, LNPs were hydrated in PBS. For zeta potential analysis, LNPs were hydrated in PBS followed by dialysis. Dialysis was required to substitute the PBS solution with distilled water. As Col II was reconstituted in acetic acid and hydrated in PBS solution, the zeta potential could be influenced by the mixed solutions. Therefore, dialysis after extrusion was necessary. To evaluate the colloidal stability of LNPs, the size variation of LNPs was monitored for 3 days by DLS. The entrapment efficiency and release profile of rapamycin in LNPs were confirmed by high performance liquid chromatography (HPLC). Briefly, the temperature of the column was maintained at 60 ℃. For the mobile phase, 10 mM ammonium acetate and acetonitrile were used (25:75, v/v). The flow rate was 1.5 ml/min and 5 μl of samples was injected for each measurement. LNP-R was destroyed with 0.1% Triton-X for 10 minutes to determine the amount of rapamycin actually loaded in LNPs. Finally, the entrapment efficiency (%) was calculated according to the following equation: (The amount of rapamycin actually loaded in LNPs/ The amount of rapamycin added to LNPs) x 100. To determine the release profile of Col II loaded in LNP-

Col II-R, bicinchoninic acid (BCA) protein assay was performed.

2.3. *In vitro* assays

2.3.1. Nanoparticle addition to DC cultures

One million DCs were seeded in each well of a 6-well plate. For nanoparticle uptake evaluation, LNPs were labeled with 1,1'-dioctadecyl-3,3,3',3'-tetramethylindocarbocyanine perchlorate (DiI) (Invitrogen™, USA), added to DC cultures, and incubated for 24 hours. DCs were washed twice with PBS and fixed with 4% paraformaldehyde (PFA). The nuclei were stained with DAPI (Vector laboratories, USA). For Col II uptake and presentation on DCs, Col II was labeled with NHS-fluorescein (FITC) (Thermo Fisher Scientific, USA) prior to addition to DC cultures. Cell cytoplasm was stained with Cell Mask™ (Thermo Fisher Scientific, USA). To detect the Eα peptide (52–68) (AnaSpec Inc., USA) on MHC II of DCs, free Eα or LNP- Eα-R treated DCs were stained with I-Ab monoclonal antibodies (Invitrogen™, USA). The staining results were examined by a confocal laser scanning microscope (LSM710, Carl Zeiss, Germany). For tDC induction, DCs were cocultured with different kinds of LNPs for 48 hours, and activated by LPS (200 ng/ml) for 24 hours. In order to mimic the in vivo inflammatory environment in OA, DCs were treated with LPS in vitro in the tDC induction studies (Fig. 2D and 2E and 2F). DCs were stained with PerCP/Cyanine 5.5-labeled anti-mouse CD40 (BioLegend, USA, 124617), PE-labeled anti-mouse CD80 (BioLegend, USA, 104707), APC-labeled anti-mouse CD86 antibodies (BioLegend, USA, 105011), and PE/cyanine5-labeled anti-mouse MHC II(BioLegend, USA, 107612) for flow cytometry analysis (FACS Aria II, BC

Biosciences, USA). At the same time, the mRNA levels of TNF-α and TGF-β in the cells were evaluated with the qRT–PCR StepOnePlus™ Real-Time PCR system (Applied Biosystems™, CA, USA). The enzyme-linked immunosorbent assay (ELISA) was conducted to measure the secretion level of TNF-α (BioLegend, USA) and TGF-β (Invitrogen™, USA) from DCs that were treated with different kinds of LNPs.

2.3.2. Antigen-specific regulatory T cells (Tregs) induction *in vitro*

For in vitro induction of antigen-specific Tregs, different kinds of LNPs were treated with DC cultures for two days followed by 200 ng/ml LPS treatment for 24 hours. The treated DCs were cocultured with CD4+ T cells isolated from OT-II transgenic mice in the presence of 2 ng/ml TGF-β for another 4 days. OT-II CD4+ T cells were isolated by magnetic-activated cell sorting (MACS) according to the manufacturer's instructions (Miltenyi Biotech, USA). After 4 days of coculture, the T cells were collected and analyzed for the expression of CD4, CD25 and Foxp3 with FACS Aria II.

2.3.3. Quantitative PCR and analysis of RNA

RNA quantity and expression were evaluated using qRT-PCR. The samples were lysed using 1 mL of the TRIzol reagent (Invitrogen, USA), and total RNA was extracted using 200 μl of chloroform. The samples were centrifuged at 10,000 g for 10 minutes at 4 ℃. The supernatant was collected, mixed with 80 % (v/v) isopropanol in water, and centrifuged at 10,000 g for 10 minutes at 4 ℃. The RNA pellet was rinsed with 75 % (v/v) ethanol, dried, and dissolved in RNase-

free water. Complementary DNA was reverse-transcribed from RNA using the AccuPower RT PreMix (Bioneer, South Korea). Gene expressions were evaluated using the SYBR green-based StepOnePlus real-time PCR system (Applied Biosystems™, CA, USA). Each cycle entained the following: 95 ℃ for 10 seconds, 60 ℃ for 15 seconds, and 72 ℃ for seconds. Glyceraldehyde 3-phosphate dehydrogenase (GAPDH) served as the housekeeping genes.

2.3.4. Evaluation of cellular viability

The numbers of viable cells were determined using the cell counting kit-8 (CCK-8) assay (EZ-CyTox, DogenBio, Korea) according to the manufacturer's instructions. The CCK-8 assay measures the amount of formazan dye that is reduced by the intracellular dehydrogenase activities. The number of living cells is proportional to the amount of the formazan dye. Briefly the DCs (1×10^4) were cultured with LNP-Col II-R nanoparticles for 24 hours, and rinsed with PBS three times. After replenishing the wells with fresh medium, CCK-8 solution was added into each well and incubated for 2 hours. The absorbance of the solution was measured at 450 nm using a spectrophotometer. The cell viability was calculated as the percentage of viable cells relative to the LNP-Col II-R-untreated cells. The mRNA levels of apoptosis related genes, BAX and Caspase-3, were determined by qRT–PCR.

2.3.5. ELSIA (enzyme-linked immunosorbent assay)

ELISA was conducted to measure the secretion level of TNF-α (BioLegend, USA)

and TGF-β (Invitrogen™, USA) from DCs. For measuring the cytokine levels from DCs, 48 hours after the treatment of nanoparticles (LNP-Col II, LNP-R, and LNP-Col II-R) to DCs, the supernatants were collected and stored at -80 ℃ until use. The experiment was conducted according to the manufacturer's instructions. Briefly, 100 μl of capture antibody was treated to each well and incubated overnight. The next day, the plate was washed for 4 times with ELISA wash buffer and 200 μl of assay diluent was treated for an hour to block non-specific binding. The plate was washed for 4 times and 200 μl of standard solutions as well as sample solutions were treated to each well and they were incubated for 2 hours. After washing the plate, detection antibody was treated for an hour. Then 100 μl of Avidin-HRP solutions was treated for 30 minutes. After washing the plate thoroughly, TMB substrate solutions were treated until the color developed from blue to yellow. The absorbance at 405 nm was measured by the 96-well microplate reader.

2.3.5. Flow cytometry

DCs were detached using a cell scraper and Trypsin-EDTA while CD4+ T cells were collected from the supernatant cell medium then they were made into single-cell suspensions. For staining surface marker of DCs, cells were stained with antibodies against CD40, CD80, CD86 and MHC II which are conjugated with peridinin chlorophyll/cyanine 5.5 (PerCP/Cy 5.5) (BioLegend, USA, 124617), phycoerythrin (PE) (BioLegend, USA, 104707), allophycocyanin (APC) (BioLegend, USA, 105011), and PE/cyanine5 (BioLegend, USA, 107612), respectively. And T cells were stained with antibodies against CD4, CD25 and Foxp3 with fluorescein isothiocyanate (FITC) (BioLegend, USA, 116003),

allophycocyanin (APC) (BioLegend, USA, 101909) and PE (BioLegend, USA, 126403). Then cells were analyzed by FACS Aria II (BD Bioscience, San Jose, CA, USA).

2.3.7. Immunocytochemistry

The cells were fixed with 4 % PFA for 15 min at room temperature and washed in PBS. Primary antibody against I-Ab was used for staining. The samples were then incubated in PBS containing streptavidin APC secondary antibodies (eBioscience, USA, 17-4317-82) for 1 hr at room temperature. All samples were mounted with mounting solution containing DAPI to stain the nuclei, and photographed using a confocal laser scanning microscope (LSM710, Carl Zeiss, Germany).

2.4. *In vivo* assays

2.4.1. OA model and treatment

Animal experiments were approved by the IACUC at Seoul National University (SNU-190426–1–3). For OA induction, 10-week-old male C57BL/6 mice (OrientBio, Gyeonggi, South Korea) were anesthetized with ketamine (200 mg/kg) and rompun (10 mg/kg). Ten-week-old mice were used because several previous animal studies involving OA used the surgically induced OA model in around 10-week-old, skeletally mature mice [21]. Male mice were used in the experiments because the incidence of post-traumatic OA model is higher in the male murine model than female models [22]. Female hormones have chondroprotective effects,

while male hormones aggravate the disease [23]. Only the right leg was operated. The skin beneath the tendon of the hind limb was opened. To secure a clear view and perform delicate operation, the whole step was performed under a microscope. The fat pad was carefully cleared, and the medial meniscus was destabilized with a No. 11 surgical blade. After destabilization, the inner wounded area was closed with coated vicryl polyglactin 910 (Ethicon, USA). The outer skin was closed with nonabsorbable black silk suture (AILEE, USA). The OA-induced mice were randomly grouped (n = 5 per group), and 2 mg of nanoparticles (42 μg rapamycin and 50 μg Col II-peptide per animal) in 100 μl PBS were injected intradermally at week 1, 2 and 6. The nanoparticles were injected intradermally because intradermal injection is simple and non-invasive and previous studies have demonstrated that intradermal injection of tolerogenic nanoparticles resulted in the induction of Tregs [24]. In dermis exist plenty of DCs, macrophages, small amount of T and B cells. Considering that macrophages in dermis do not migrate via lymph vessels to adjacent lymph nodes and rapamycin do not directly polarize macrophages towards anti-inflammatory M2 macrophages, the ability of dermal macrophages as antigen presenting cells is negligible [25]. Thus DCs play a pivotal role in delivering antigen and inducing antigen-specific Tregs. To ameliorate the initial inflammation induced by inflammatory M1 macrophages and effector T cells after DMM surgery, the nanoparticles were injected at weeks 1 and 2. The nanoparticles were injected again at week 6 to boost the induction of Col II-specific Tregs. For sham surgical group, only the skin of the right leg was incised and no further procedures were conducted. In previous studies, DMM-induced mice were sacrificed between 4 and 12 weeks [26] and mostly at 8 weeks for therapeutic effect evaluation [27]. Considering that synovial inflammation does not occur in very early stage of OA, we excluded early time points for animal

sacrifice and assessed the therapeutic effects at 8 weeks.

2.4.2. *Ex vivo* biodistribution of LNP-Col II-R

LNP-Col II-R nanoparticles were labeled with 1,1′-dioctadecyl-3,3,3′,3′-tetramethylindotricarbocyanine iodide (DiR) (AAT Bioquest, USA). Briefly, DiR iodide in ethanol at 1 mg/ml was added to the nanoparticle stock solution. DiR-labeled LNP-Col II-R in 100 μl PBS was injected intradermally into mice. The biodistribution was evaluated by an IVIS spectrum instrument (IVIS® SpectrumCT, Perkin Elmer, USA). To examine the interaction between DCs and LNP-Col II-R in vivo, LNP-Col II-R nanoparticles were labeled with 1,1′-dioctadecyl-3,3,3′,3′-tetramethylindodicarbocyanine (DiD) (Invitrogen™, USA) and injected intradermally into mice. iLNs were harvested 24 hours after injection and cryosectioned. DCs in the iLNs were stained with CD11c antibodies (Abcam, USA, ab33438) and CD3 antibodies (Abcam, USA, ab5690). The coexistence of CD11c-positive cells with DiD-labeled LNPs or CD11c and CD3-positive cells with DiD-labeled LNPs were analyzed with confocal microscopy.

2.4.3. Antigen-specific Treg induction *in vivo*

Different kinds of LNPs were injected intradermally near the right iLN of OT-II transgenic mice, where CD4+ T cell receptors are specifically responsive to chicken $OVA_{323-339}$. The study with OT-II transgenic mice was approved by the Institutional Animal Care and Use Committee (IACUC) at Seoul National University (SNU-190726). Four days after injection, lymph nodes were harvested and minced for Treg analysis. The gathered cells were stained with mouse anti-

CD4-fluorescein isothiocyanate (FITC) (BioLegend, USA, 116003) and mouse anti-CD 25-allophycocyanin (APC) antibodies (BioLegend, USA, 101909) for 30 minutes at 4 ℃. For intracellular Foxp3 staining, the cells were permeabilized with Fix/Perm buffer (eBioscience, USA) for 30 minutes at 4 ℃, washed with permeabilization buffer (eBioscience, USA) and stained with mouse anti-Foxp3-phycoerythrin (PE) antibodies (BioLegend, USA, 126403) for 30 minutes at 4 ℃. The cells were analyzed with an automated high-speed flow cytometry system (FACS Aria II, BD Biosciences, USA). For the induction of antigen-specific Tregs in wild-type mice, DMM surgery was conducted, and different kinds of LNPs were treated once a week, 3 times in total. Four days after the 3rd injection, splenocytes were harvested and seeded in 24-well plates ($1x10^6$ cells/well). Antigens (12.5 μg/ml) were treated, and the cells were harvested after 72 hours. The cells were stained with anti-CD4, anti-CD25 and anti-Foxp3 antibodies, and the proportion of CD4+CD25+Foxp3+ Tregs was analyzed with FACS Aria II. The mRNA levels of anti-inflammatory cytokines (Foxp3, and TGF-β) were analyzed with qRT–PCR.

2.4.4. Autoantibody level against type II collagen in blood serum

For measuring the level of autoantibodies against type II collagen in DMM-induced murine OA model, blood was drawn by intraorbital vein blood collection method using capillary tubes. Serum was isolated from the whole blood by centrifuging the blood at 800 g for 13 minutes twice. The serum samples were stored at -80 ℃ until use. The level of autoantibodies against type II collagen was measured by ELISA and the experiment was conducted according to the manufacturer’s instruction.

2.4.5. Histology and immunohistological assessment *in vivo*

The joints were harvested 8 weeks after surgery, fixed with 4% PFA for 24 hours, and decalcified in decalcifying solution-Lite (Sigma Aldrich, USA) for 5 days. The samples were embedded in paraffin and serially sectioned frontally at 3-μm thickness using a microtome (Leica RM2125, Germany). For Safranin O-Fast Green staining, the sections were stained with 0.1% Safranin O solution and 0.05% Fast Green solution, mounted with Canada balsam (Sigma Aldrich, USA) and examined with a microscope (Olympus IX71–22FL/PH, Tokyo, Japan). The stained images were scored by the OARSI scoring method by four observers who were blind to the animal groups and three slides per joint were used to generate each data point. For assessment of synovitis, the slides were stained with Harris Hematoxylin (Cancer Diagnostics Inc, USA) and Clearview™ Eosin (BBC Biochemical, USA). Immunostaining for collagen type II alpha 1 chain (Col2a1) and MMP13 were performed using the Envision Detection kit (DAKO Agilent Technologies, Inc., USA). Sections were stained with primary antibodies against Col II (Abcam, USA, ab34712) and MMP13 (Abcam, USA, ab3208) at 4 ℃ overnight, and incubated with EnVision/HRP for 30 minutes. The final-colored products were developed using chromogen diaminobenzidine (DAB) and examined under a microscope (Leica Biosystems, Nussloch, Germany). For immunostaining for Tregs, M1 macrophages, and M2 macrophages, tissue sections were stained with anti-CD4-Alexa Fluor® 488 (Invitrogen, USA, A-11006), anti-CD25-allophycocyanin (APC) (BD Pharmingen, USA, 550874), anti-Foxp3 (NOVUS, USA, NB100–39002), anti-F4/80 (Abcam, USA, ab16911), anti-iNOS (Abcam, USA, ab15323) and anti-arginase (NOVUS, USA, NBP1–

32731) antibodies. After overnight incubation at 4 ℃, the sections were incubated with goat anti-rabbit IgG secondary antibody-PE (SouthernBiotech, USA, 4050–09), goat anti-mouse IgG secondary antibody-Alexa Fluor 555 (Invitrogen, USA, A-21127), and goat anti-rabbit IgG secondary antibody-FITC (NOVUS, USA, NB7182). For immunostaining of IFN-γ-secreting CD4+ T cells, IL-17-secreting CD4+ T cells, IL-1β-secreting M1 macrophages, and IL-10-secreting Tregs, tissue sections were stained with anti-CD4 (NOVUS, USA, NBP2–25191), anti-F4/80 (Abcam, USA, ab16911), anti-Foxp3 (NOVUS, USA, NB100–39002), anti-IL-1β (NOVUS, USA, NB600–630, anti-IL-17 (Abcam, USA, ab79056), anti-IFN-γ (Invitrogen, USA, 12–7311–82) and anti-IL-10 (Abcam, USA, ab189392) antibodies. The staining was visualized by confocal microscopy (LSM 700 Meta, Carl Zeiss, Oberkochen, Germany).

2.4.6. Apoptosis assessment *in vivo*

Deoxynucleotidyl transferase dUTP nick end labeling (TUNEL) assay was performed to detect apoptotic cells with the in situ cell death detection kit (Roche). Briefly, fixed joint sections were permeabilized and incubated with fluorescein TUNEL reaction mixture containing for 60 min at 37℃ in dark. After washing with PBS, nuclei were stained with DAPI and the samples were photographed using confocal microscope.

2.4.7. Whole joint PCR

mRNA levels of inflammatory and anti-inflammatory cytokines in the joints were analyzed. The joint tissues including synovium, femoral condyle and tibial plateau

were harvested, and unnecessary tissues were trimmed as much as possible. The excised tissues were minced with a blade and then homogenized thoroughly. Before homogenization, TRIzol was added, and the samples were stored at -80 ℃ until use. mRNA levels of TNF-α, TGF-β, IL-1β and IFN-γ were evaluated with qRT-PCR.

2.4.8. Pain evaluation

The pain evaluation was conducted 8 weeks after surgery. For the mechanical allodynia test, each animal was acclimatized in a single chamber for at least 30 minutes. An electronic von Frey device (Dynamic Plantar Aesthesiometer, Ugo Basile, Italy) was placed beneath the animals, and the filaments pressed the footpad of the animals successively starting from lower force. The point at which the animals felt pain and removed their foot from the plate was recorded. For the static weight-bearing test, each animal was acclimatized in the chamber for at least 5 minutes. Both forelegs were forced up against the wall of the chamber, and only the hind limbs were placed on each right and left weighing machine (Incapacitance Meter, IITC Life Science, USA). The results recorded on both sides of the weighing machine were analyzed. The greater the pain perception of the animals, the faster they removed their foot from the plate.

2.4.9. Adoptive transfer of Tregs to OA mice

CD4+CD25+ T cells were isolated from the spleens of OA mice that had been treated with intradermal injection of PBS, LNP-R, or LNP-Col II-R at weeks 1 and 2. The isolated splenocytes were stained with anti-CD4 fluorescein

isothiocyanate (FITC) (BD Pharmingen, USA, 45-0042-82) and anti-CD25 allophycocyanin (APC) (BioLegend, USA, 102012) for 30 minutes at 4 ℃ in the dark. CD4+CD25+ T cells were sorted by Moflo (Beckman Coulter, Brea, CA, USA). The sorted CD4+CD25+ Tregs ($0.5x10^6$ cells per animal) were transferred to OA mice through intravenous injection. Eight weeks after Treg transfer, the joints were harvested for analysis.

2.4.10. Adoptive transfer of DCs to OA mice

CD11c+ DCs were isolated from the right inguinal lymph nodes of wild type mice that had been treated with intradermal injections of PBS, LNP-R, or LNP-Col II-R on week 1 and week 2. The isolated lymphocytes were stained with anti-CD11c Microbeads Ultrapure (Miltenybiotec, USA, 130-125-835) for 15 minutes and sorted by MACS bead column according to manufacturer's instruction (Miltenyi Biotech, USA). The sorted CD11c+ DCs ($0.5x10^6$ cells per animal) were transferred to OA mice through intradermal injection. Eight weeks after DC transfer, the joints were harvested for analysis.

2.4.11. Evaluation of in vivo toxicity

For in vivo organ toxicity analysis, 2 mg of LNP-Col II-R nanoparticles were intradermally injected into mice. At various time points, blood serum samples were isolated, and the blood levels of ALT, AST, BUN and creatinine were determined by a veterinary automatic dry chemistry analyzer (DRI-CHEM 3500s, Fuji, Japan). At week 8, major organs, including the heart, liver, lung, kidney and spleen were harvested and processed for histological examination with H&E

staining method.

2.5. Statistical analysis

All quantitative data are expressed as the mean ± standard deviation. Two-tailed Student's t-test was used for comparison between two groups. A one-way analysis of variance (ANOVA) followed by Tukey's test was used for all statistical analysis. A difference with a P value less than 0.05 was considered statistically significant. All statistical analyses were performed using Prism 8.0 (GraphPad Software Inc.).

Chapter 3.

Nanoparticle-mediated induction of type II collagen-specific regulatory T cells for osteoarthritis treatment

3.1. Introduction

Osteoarthritis (OA) is a common joint disease that involves cartilage destruction and subchondral bone sclerosis, and is accompanied by severe pain and locomotion limitations. The general treatments for OA prior to joint replacement include oral administration of nonsteroidal anti-inflammatory drugs (NSAIDs) and injection of hyaluronic acid within the joint [9]. However, these treatments relieve symptoms only to a certain extent, cannot stop the progression of the disease, and often cause side effects. Autologous chondrocyte implantation can be used to regenerate cartilage in OA patients [10], but is costly and invasive.

OA has been traditionally considered a noninflammatory disease caused by mechanical wear of cartilage. However, recent emerging evidence has indicated that inflammation in the synovium (synovitis) also contributes to OA development [28, 29]. Low-grade chronic inflammation in OA is initiated by mechanical wear of cartilage and sustained via innate and adaptive immune responses [4]. Mechanical wear of cartilage leads to the release of extracellular matrix (ECM) fragments and damage-associated molecular patterns (DAMPs), which induce innate immune responses such as the release of proinflammatory mediators and macrophage infiltration into OA synovium [30]. Compared to the synovium of healthy individuals, that of OA patients contains higher numbers of inflammatory immune cells, such as M1 macrophages, type 1 helper T cells (Th1 cells) and type 17 helper T cells (Th17 cells), and lower numbers of anti-inflammatory regulatory T cells (Tregs) [6, 29, 31, 32, 33]. Inflammatory immune cells propagate synovitis and further deteriorate the cartilage tissue. T cells isolated from OA patients induced autoimmune responses to autologous articular chondrocytes in vitro [34]. Clonal expansion of antigen-specific B cells was found in

patients' OA synovium [35]. Furthermore, autoantibodies against cartilage-derived molecules, such as Col II, proteoglycan and aggrecan, were found in sera and synovial fluids of OA patients [8, 32, 36]. These results suggest that OA is a multi-antigenic inflammatory disease and could be effectively treated by antigen-specific immune modulation in the joint.

Tregs can inhibit inflammatory immune cells such as M1 macrophages and Th1 cells through secretion of anti-inflammatory cytokines [e.g., interleukin-10 (IL-10) and transforming growth factor-β (TGF-β)] [37, 38]. Thus, adoptive Treg transfer therapy may hold great promise for treating inflammatory diseases [39]. For the therapy, Tregs specific for a desired antigen would be advantageous over polyclonal Tregs for the following reasons. First, adoptive transfer of polyclonal Tregs may cause side effects of non-specific systemic immune suppression through systemic secretion of anti-inflammatory cytokines [39, 40]. Non-specific systemic immune suppression may increase vulnerability to life-threatening infections and the risk of developing malignancies. Tregs specific for a desired antigen exert more localized and targeted immune suppression than polyclonal Tregs. Second, antigen-specific Tregs have been proven to be functionally superior to polyclonal Tregs in animal models [41, 42]. This would be ascribed to localization and activation of antigen-specific Tregs at the target site through interactions with antigen presented by antigen-presenting cells at the inflammation site. However, broad clinical applications of adoptive transfer of autologous Tregs would be limited by the costly and complicated procedures of ex vivo Treg manufacturing [39]. In this context, in vivo induction of OA antigen-specific Tregs may show potential for OA treatment and may be advantageous over adoptive transfer of OA antigen-specific Tregs or polyclonal Tregs.

Here, we present an off-the-shelf approach for OA treatment, which involves nanoparticle-mediated in vivo induction of Col II-specific Tregs (Figure 3.1.). In vivo induced Col II-specific Tregs may ameliorate inflammation at the OA joint and inhibit OA progression. Col II was selected as the antigen for induction of antigen-specific Tregs. Col II is a major component of cartilage ECM and a potential autoantigen since autoantibodies against Col II are found in the synovial fluid and serum in OA patients [7]. Col II present in the OA joint is susceptible to modification by inflammatory molecules, such as proteolytic enzymes and reactive oxygen species [43], and the modification potentially increases its antigenicity [32, 34, 35, 44, 45, 46]. Thus, we used Col II that was degraded by a proteolytic enzyme as the antigen to induce Col II-specific Tregs. The hypothesis of our approach (Fig. 1A) is as follows. Intradermally injected lipid nanoparticles (LNPs) loaded with Col II and rapamycin (LNP-Col II-R) are taken up by dendritic cells (DCs). DCs subsequently differentiate into tolerogenic DCs (tDCs) due to rapamycin, present Col II on major histocompatibility complex (MHC) class II, migrate to adjacent lymph nodes and induce Col II-specific Tregs. Col II-specific Tregs migrate to the site of inflammation (i.e., OA joint) and are activated upon interaction with Col II presented on MHC class II of antigen-presenting cells (e.g., activated B cell, DC and macrophage) at the OA synovium. The activated Tregs ameliorate joint inflammation. We tested this hypothesis in a murine OA model.

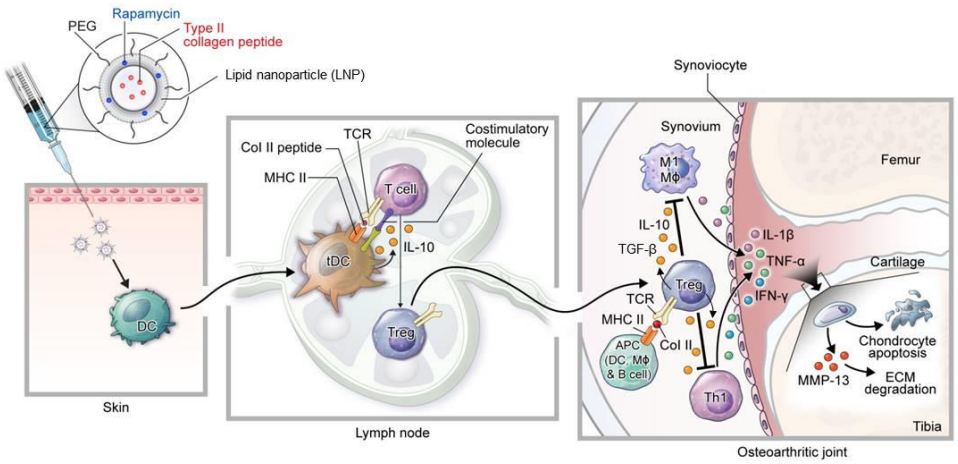

Figure 3.1. The hypothesis of this study. Intradermal injection of LNP-Col II-R to osteoarthritis (OA) mice would induce Col II-specific regulatory T cells (Tregs). The Tregs in the synovium would inhibit M1-type macrophages (M1 macrophages) and type 1 helper T cells (Th1 cells) both of which express inflammatory cytokines [e.g., (tumor necrosis factor-α) TNF-α, (interferon-γ) IFN-γ, and (interleukin-1β) IL-1β] and inhibit chondrocyte apoptosis and matrix destruction in the OA articular cartilage.

3.2. Results and discussion

3.2.1. Characterization of LNP-Col II-R

Col II for LNP-Col II-R was prepared through collagenase treatment of undenatured Col II proteins. The molecular weights of undenatured Col II proteins ranged from 13 to 100 kDa, while those of Col II after collagenase treatment ranged from 6 to 16 kDa (Figure 3.2.). LNP-Col II-R exhibited a round morphology (Figure 3.3A) and an average size of 215.4 ± 53.8 nm (Figure 3.3B).

LNP-Col II-R showed a positive surface charge of 6.2 ± 3.6 mV due to the cationic lipid DOTAP of LNP. Differential scanning calorimetry (DSC) analysis revealed incorporation of rapamycin in LNP-Col II-R (Figure 3.3C). The thermogram of free rapamycin crystals showed an endothermic peak at ~190 ℃ [47]. The peak was not observed in rapamycin-loaded LNPs (LNP-R and LNP-Col II-R) or in blank LNPs, indicating that rapamycin was incorporated into LNPs and existed in an amorphous state in the lipid bilayer of the LNPs. High-performance liquid chromatography (HPLC) analysis confirmed that rapamycin was loaded in LNP-Col II-R (Figure 3.3D). The rapamycin loading efficiency was 65.9%. Confocal microscopic analysis revealed that Col II was incorporated in LNPs (Figure 3.3E). LNP-Col II-R showed colloidal stability in 50% (v/v) serum for at least 3 days (Figure 3.3F). Considering that DCs engulf nanoparticles within 24 h after intradermal injection [48, 49], LNP-Col II-R that are stable for 3 days would be appropriate for DC uptake after intradermal injection. Less than only 10 % of rapamycin and Col II peptides were released from LNP-Col II-R within 72 hours (Figure 3.3G). The slow release profiles ensure that the payloads (rapamycin and Col II) are released intracellularly. LNP-Col II-R can be internalized into endosomes of DCs by endocytosis. Subsequently, the payloads are released to the cytosol via LNP fusion with endosomal membranes [50, 51]. The fusion is mediated by the interactions between cationic lipids of LNPs and anionic endosomal membranes. The intracellular release leads to induction of Col II-presenting tDCs [52]. In this context, the design of nanoparticles would be appropriate for induction of tDCs.

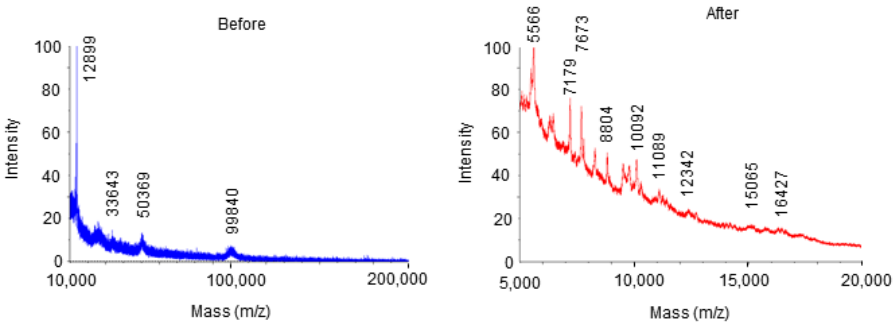

Figure 3.2. MALDI-TOF (matrix-assisted laser desorption/ionization time-of-flight) mass spectrometry data of type II collagen. The molecular weights of type II collagen proteins were measured before and after treatment with collagenase.

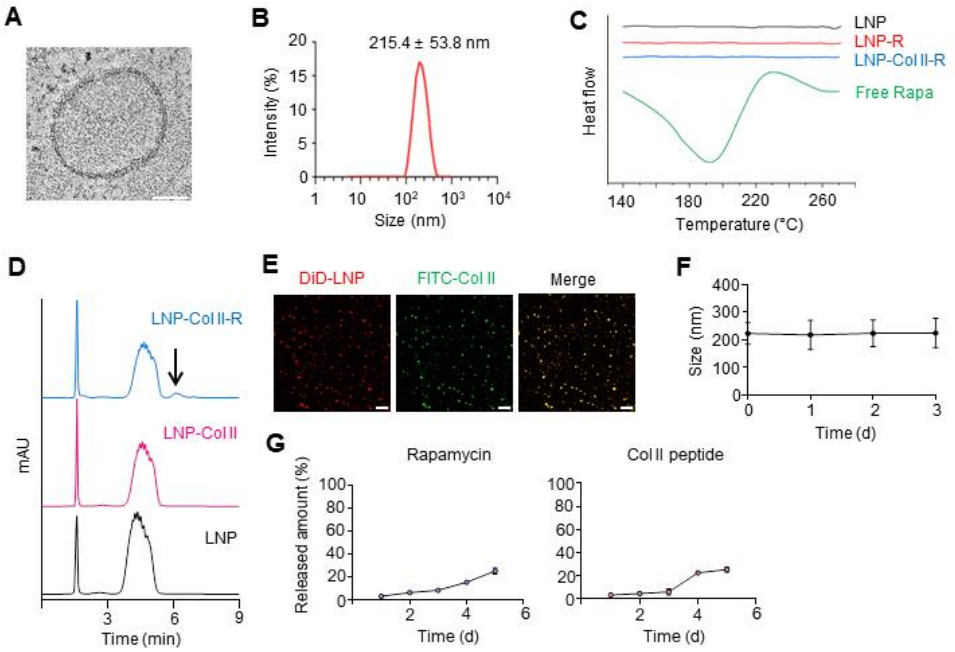

Figure 3.3. Characterization of lipid nanoparticles (LNPs) loaded with type II collagen peptide (Col II) and rapamycin (LNP-Col II-R). (A) Transmission electron microscopy (TEM) image and (B) size distribution of LNP-Col II-R. Scale bar = 50 nm. Confirmation of rapamycin loaded in LNP, as evaluated by (C) differential scanning calorimetry (DSC) and (D) high-performance liquid chromatography (HPLC). Arrow indicates rapamycin peak. (E) Confirmation of Col II loaded in LNP by confocal microscopic photographs of LNP-Col II-R. Scale bars = 1 μm. (F) Colloidal stability of LNP-Col II-R in 50 % (v/v) serum, as evaluated by dynamic laser scattering (DLS) (n = 3). (G) Confirmation of released amount of Col II peptide and rapamycin from LNP-Col II-R by bicinchoninic acid (BCA) protein assay and HPLC, respectively (n = 3).

3.2.2. Cellular uptake of LNP-Col II-R *in vitro*

To determine whether LNPs enhance Col II (antigen) delivery to DCs and subsequent antigen presentation on DCs compared to free Col II or LNP-Col II-R was added to DC cultures. After 24 hours, 91.8% of the DCs engulfed the LNPs (Figure 3.4A). In addition, LNP-Col II-R enhanced Col II delivery to DCs compared with free Col II (Col II-bearing DCs: 93.3% versus 2.2%) (Figure 3.4B). Most of the Col II was presented on the DC surface in the LNP-Col II-R injection group. To determine whether antigen delivery with LNPs leads to antigen presentation on MHC II of DCs, LNPs were loaded with Eα peptides and rapamycin, and then added to DC cultures. Technically, the presentation of Col II on MHC II of DCs is difficult to prove directly. Thus, we exploited the Yae antibodies that bind to both the Eα peptide and MHC II simultaneously, and indirectly demonstrated Eα peptide (antigen) presentation on MHC II following the addition of LNP-Eα-R to DC cultures (Figure 3.4C). The addition of LNP-Eα-R led to 82.0% of the DCs presenting Eα peptide on MHC II. In contrast, the addition of free Eα peptides to DC cultures resulted in only 17.1% of the DCs presenting Eα peptide on MHC II.

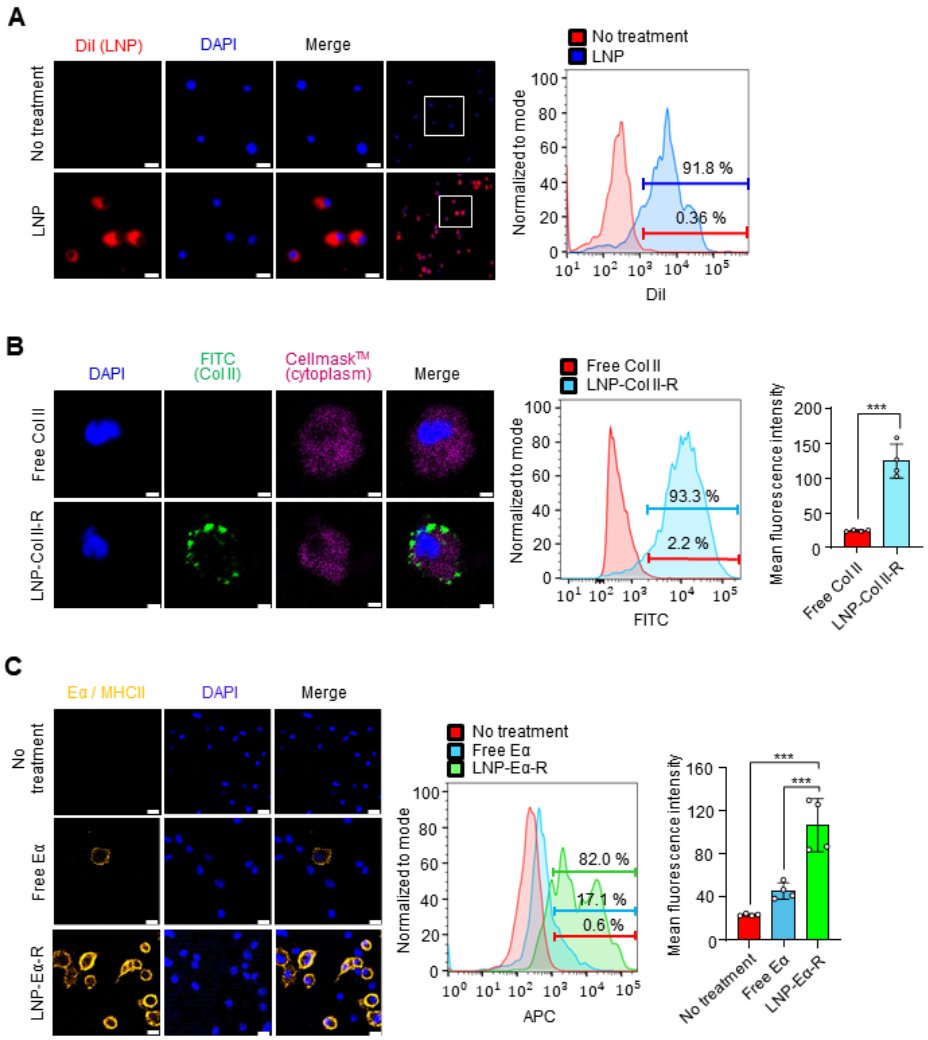

Figure 3.4. LNP-Col II-R-mediated antigen presentation on dendritic cells (DCs). (A) Effective uptake of LNPs by DCs in vitro. Scale bars = 50 µm. (B) LNP-Col II-R-mediated, effective presentation of antigen (Col II) on DCs in vitro. Scale bars = 10 µm. (n = 4). (C) LNP-mediated, effective presentation of antigen (Eα peptide) on major histocompatibility complex class II (MHC II) of DC surface in vitro. Scale bars = 50 µm. (n = 4). (B) ***p<0.001. two–tailed *t* test. (C)

***p<0.001. One way ANOVA (multiple comparison) with Tukey's post hoc test.

3.2.3. Induction of tolerogenic DCs (tDCs) *in vitro*

tDC can induce naïve T cells to differentiate into Tregs. To determine whether LNP-Col II-R can induce tDCs, DCs were cultured in the presence of different types of LNPs for 48 hours and subsequently activated by LPS for 24 hours. Rapamycin, an immunosuppressive agent, is known to endow DCs with tolerogenic properties [52]. Flow cytometry analysis indicated that mature DCs (mDCs) expressed costimulatory surface molecules (CD40, CD80, CD86) and MHC II at higher levels than immature DCs (iDCs) (Figure 3.5A). The costimulatory molecule levels of LNP-Col II-R- and LNP-R-treated DCs were significantly higher than those of iDCs and lower than those of LNP-Col II-treated DCs and mDCs. qRT–PCR analysis showed that mDCs expressed the highest mRNA levels of inflammatory cytokine, tumor necrosis factor- α (TNF-α), and the lowest mRNA level of anti-inflammatory cytokine, TGF-ß, compared with the other groups (Figure 3.5B). The mRNA level of TNF-α in LNP-Col II-R-treated DCs was higher than that of iDCs and lower than those of LNP-Col II-treated DCs and mDCs. The TGF-ß mRNA level of LNP-Col II-R-treated DCs was significantly higher than those of iDCs, LNP-Col II-treated DCs and mDCs. Together, these data indicate that LNP-Col II-R treatment to DCs can induce tDCs. The ELISA data showed that LNP-Col II-R treated DCs secreted more anti-inflammatory cytokine (TGF-β) than iDCs and mDCs, and less inflammatory cytokine (TNF-α) than mDCs (Figure 3.5C).

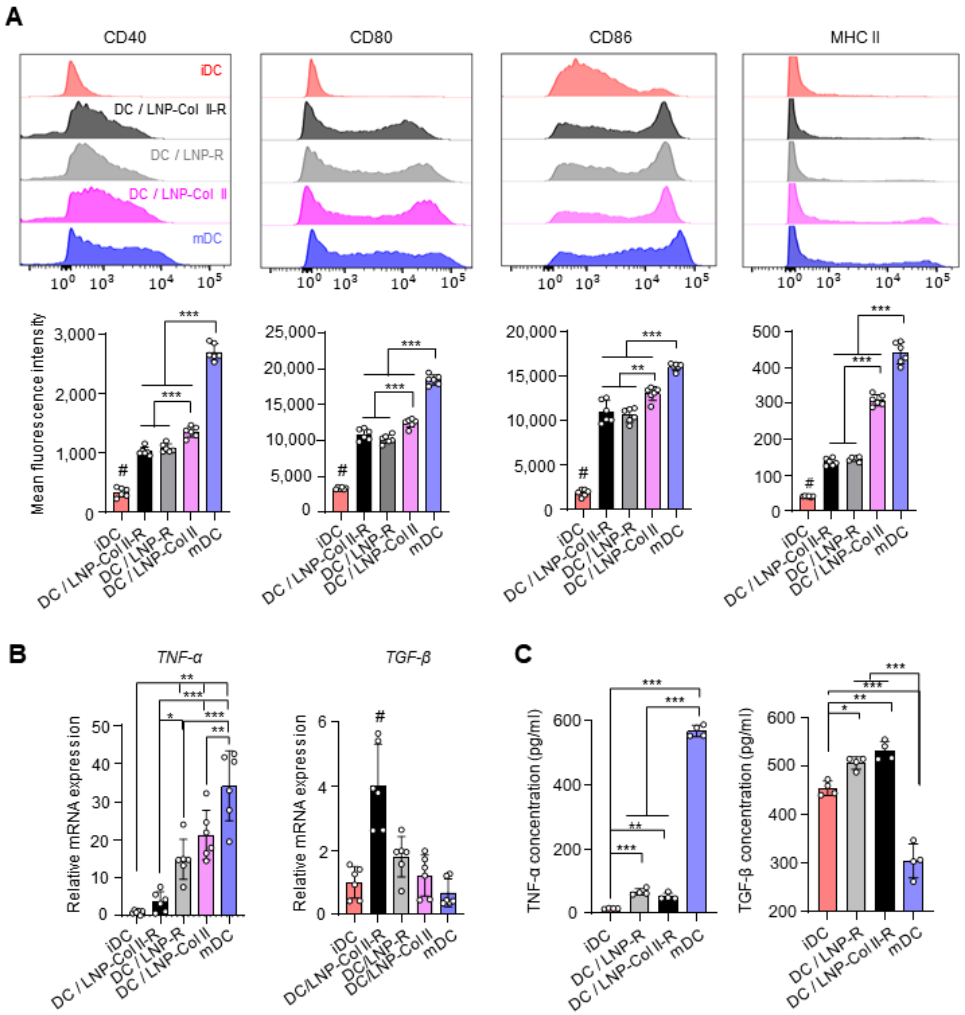

Figure 3.5. LNP-Col II-R-mediated induction of tolerogenic dendritic cells (tDCs) in vitro. LNP-Col II-R-mediated, effective induction of tDCs in vitro, as evaluated by DC surface protein analyses with (A) flow cytometry (n = 6), (B) cytokine mRNA analysis with qRT-PCR (n = 6) and (C) ELISA (n = 4). (A), (B) and (C) #p<0.001 versus any group, *p<0.05, **p<0.01, ***p<0.001. One way ANOVA (multiple comparison) with Tukey's post hoc test.

3.2.4. Antigen-specific Treg induction *in vivo* and *in vitro*

Given that LNP-R can induce tDCs (Figure 3.5A, 3.5B and 3.5C), we next investigated whether LNP-antigen-R can induce antigen-specific Tregs both in vivo and in vitro. Considering that CD4+ T cells of OT-II transgenic mice are highly responsive to chicken ovalbumin 323–339 peptide (OVA), LNPs loaded with different types of molecules were injected intradermally into OT-II mice in order to assess the ability of LNPs loaded with OVA to induce OVA-specific Tregs in vivo (Figure 3.6A). LNP-OVA-R injection resulted in a significantly higher proportion of OVA-specific Tregs in the iLNs than the other types of nanoparticles including LNP-R, LNP-Col II-R and LNP-OVA. Next, we evaluated the ability of DCs harboring LNP-antigen-R nanoparticles to activate and expand antigen-specific Tregs in vitro (Figure 3.6B). DCs were treated with different types of LNPs in vitro and subsequently cocultured with CD4+ T cells isolated from OT-II transgenic mice. The LNP-OVA-R group showed significantly higher activation of Tregs than the other groups. Next, we investigated whether intradermal injection of LNP-Col II-R generates Col II-specific Tregs in OA wild-type mice. LNPs loaded with different types of molecules were injected into the mice. Then, splenocytes were harvested and treated with Col II or OVA for antigen-specific restimulation. The LNP-Col II-R group restimulated with Col II showed the highest proportion of Tregs (Figure 3.6C) and the highest mRNA expressions of Treg-specific genes, forkhead box p3 (Foxp3) and TGF-β (Figure 3.6D). The well-known epitope for Col II is Col $II_{259-273}$. Col $II_{259-273}$ is known to be loaded on MHC II and aggravate rheumatoid arthritis by activating Col $II_{259-273}$-specific CD4+ T cells [53]. We examined the feasibility of Col $II_{259-273}$ epitope for in vivo generation of Col $II_{259-273}$-specific Tregs. After intradermal injection of LNP-Col $II_{259-273}$-R or LNP-OVA-R to mice, splenocytes were harvested and

treated with Col $II_{259-273}$ or OVA in vitro for Treg restimulation. The LNP-Col $II_{259-273}$-R group showed the highest proportion of Tregs (Figure 3.6E). Collectively, these data indicate that LNP-Col II-R can generate Col II-specific Tregs.

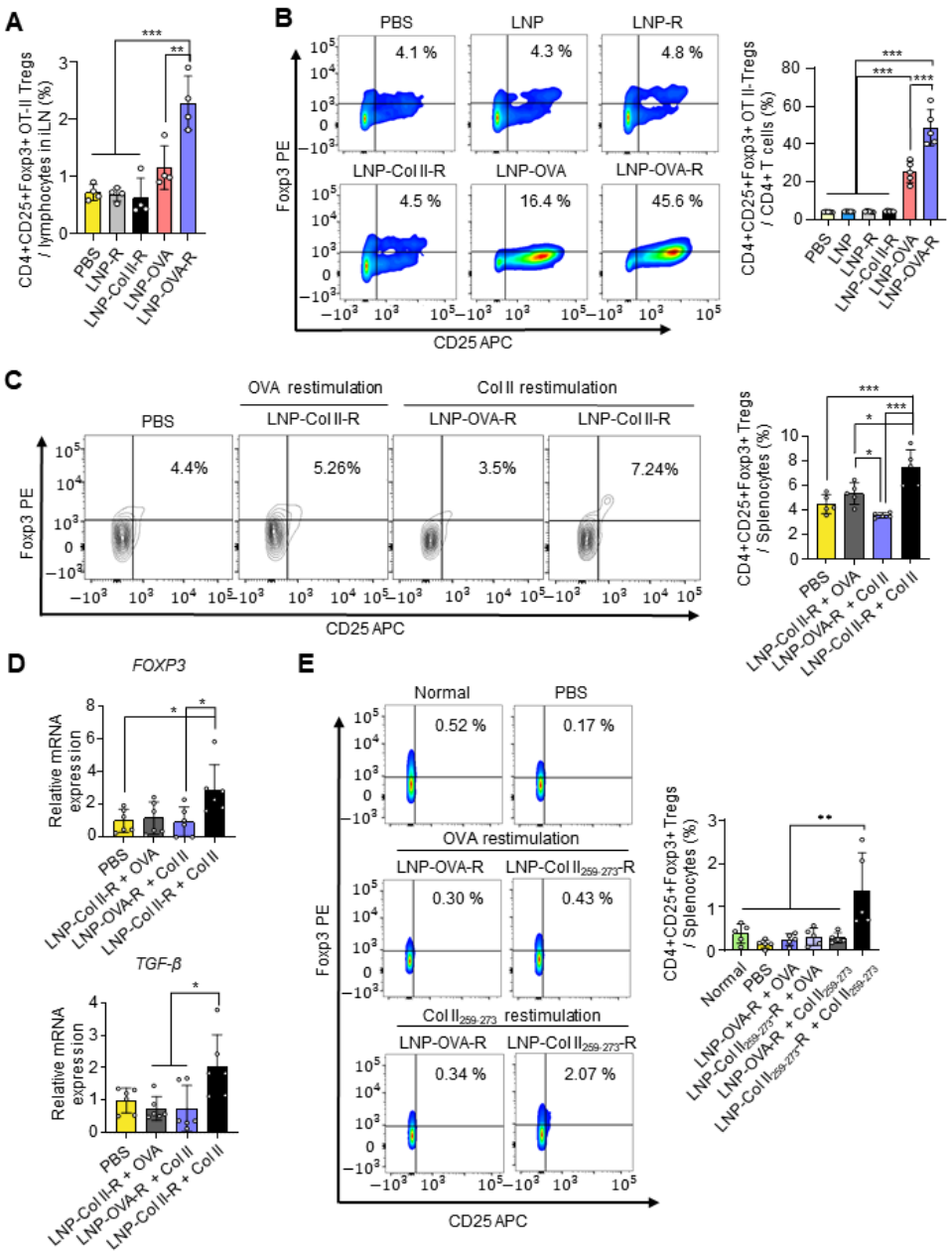

Figure 3.6. In vitro and in vivo generation of antigen-specific Tregs by

nanoparticles. (A) The proportion of OVA-specific Tregs in iLN following intradermal injection of different types of nanoparticles to OT-II transgenic mice that have T cells specific for OVA only, as evaluated by flow cytometry. (n = 4). (B) The proportion of Tregs generated in vitro from OT-II CD4+ T cells following coculture of the CD4+ T cells with DCs that had been treated with various types of nanoparticles in vitro. (n = 5). (C) The proportion of Tregs in splenocytes. The splenocytes were isolated from wild-type OA mice that had been treated with intradermal injection of different types of nanoparticles, and subsequently restimulated in vitro with Col II or OVA. (n = 5). (D) The relative mRNA expression of FOXP3 and TGF-β in the splenocytes restimulated in vitro with Col II or OVA. (n = 6). (E) The proportion of Tregs in splenocytes analyzed by flow cytometry. The splenocytes were isolated from wild-type OA mice that had been treated with intradermal injection of different types of nanoparticles, and subsequently restimulated in vitro with Col $II_{259-273}$ (epitope) or OVA. (n = 5). (A-E) *$p<0.05$, **$p<0.01$, ***$p<0.001$. One way ANOVA (multiple comparison) with Tukey's post hoc test.

3.2.5. Biodistribution of LNP-Col II-R *in vivo*

To examine the biodistribution of LNP-Col II-R after intradermal injection, LNPs were labeled with DiR, a lipophilic dye, and then intradermally injected near the right inguinal lymph node (iLN) of mice. In vivo imaging at 6, 24, and 48 hours after injection revealed that the nanoparticles existed near the injection site for at least 48 hours (Figure 3.7A). DCs are known to engulf foreign particles within 24 hours [48, 49]. At 24 hours, the DiR-labeled nanoparticles were observed only in the right iLNs and not in the major organs (Figure 3.7B). The in vivo biodistribution study of free rapamycin could not be conducted because it is difficult to label rapamycin with fluorescent dye. Instead, we conducted a biodistribution study using a fluorescent molecule, DiR, which has a similar hydrophobic property to that of rapamycin. Free DiR molecules dispersed in vivo after intradermal injection near the right inguinal lymph node, and fluorescence was not detected near injection site 2 hours after injection and in the major organs and the right inguinal lymph node 24 hours after injection (Figure 3.7C and 3.7D). These results suggest that intradermal injection of free rapamycin might not be suitable for local delivery to lymph node. Immunostaining of the right iLNs retrieved at 24 hours revealed that DCs (CD11c+ cells) contained LNPs (Figure 3.7E) and interacted with CD3+ T cells in paracortex of the lymph node (Figure 3.7E and 3.7F).

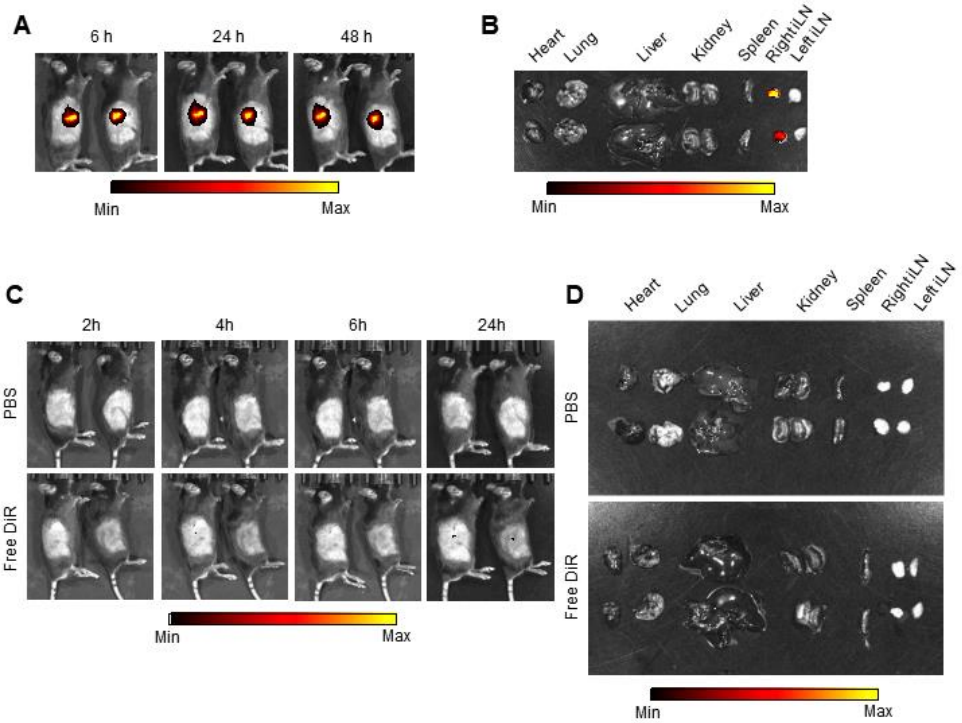
A
6 h
24 h
48 h
Min
Max
B
Heart
Lung
Liver
Kidney
Spleen
RightiLN
LeftiLN
Min
Max
C
2h
4h
6h
24h
PBS
Free DiR
Min
Max
D
Heart
Lung
Liver
Kidney
Spleen
RightiLN
LeftiLN
PBS
Free DiR
Min
Max

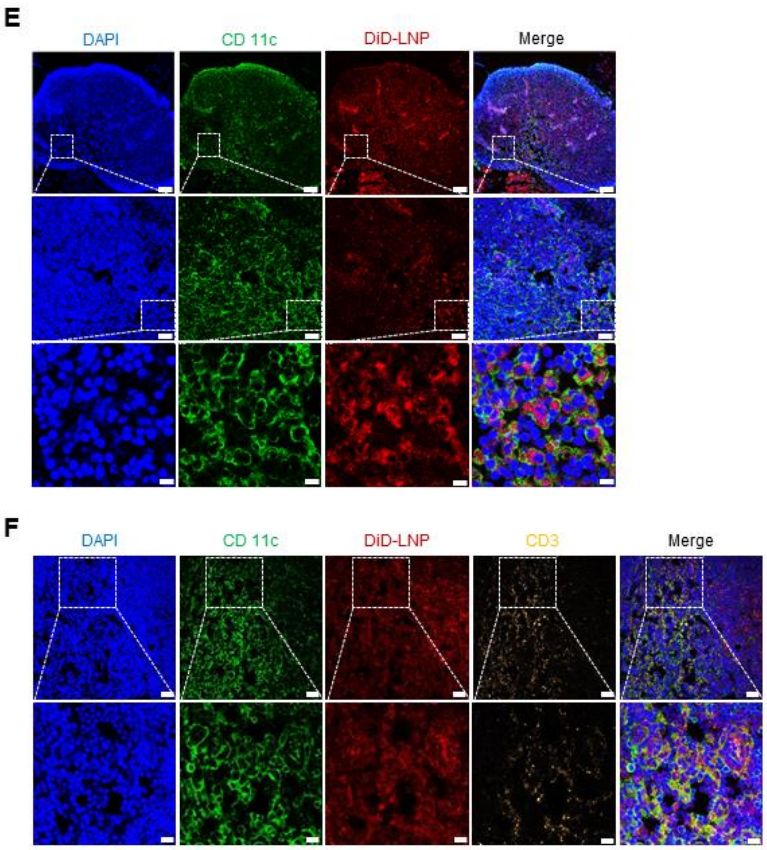

Figure 3.7. Biodistribution of LNP-Col II-R after intradermal injection. (A) The fluorescence intensity of 1,1′-dioctadecyl-3,3,3′,3′-tetramethylindotricarbocyanine iodide (DiR)-labeled LNP-Col II-R at 6, 24 and 48 hours after intradermal injection near the right inguinal lymph node (iLN) of mice. (B) The fluorescence intensity of major organs and iLN 24 hours after intradermal injection near the right iLN. The fluorescence intensity of DiR of (C) mice at 2, 4, 6 and 24 hours after intradermal injection of PBS or free DiR near the right inguinal lymph node (iLN), and (D) the major organs and iLN after 24 hours of injection. (E) Immunostaining of DCs in the right iLN with anti-CD11c antibodies 24 hours after intradermal injection of 1,1′-dioctadecyl-3,3,3′,3′-

tetramethylindodicarbocyanine (DiD)-labelled LNP-Col II-R, indicating co-localization of LNP-Col II-R and DCs in the right iLN. The photographs of the lowest row are a higher magnification of the rectangular areas (paracortex) of those in the upper rows. Scale bars in the most upper row, middle row and lowest row are 100, 50 and 5 μm, respectively. (F) Immunostaining of DCs and T cells in the right iLN with anti-CD11c and anti-CD3 antibodies 24 hours after intradermal injection of 1,1′-dioctadecyl-3,3,3′,3′-tetramethylindodicarbocyanine (DiD)-labelled LNP-Col II-R, indicating co-localization of LNP-Col II-R, DCs and T cells in the right iLN. The photographs of the lower row are a higher magnification of the rectangular areas of those in the upper row. Scale bars in the upper row and lower row are 50 and 10 μm, respectively.

3.2.6. Chondroprotective effects of LNP-Col II-R *in vivo*

To evaluate the therapeutic effects of LNP-Col II-R, C57BL/6 mice underwent destabilization of medial meniscus (DMM) surgery on the right side of the knee for OA induction, and the left knee remained as a control [54]. The level of autoantibodies against Col II in murine DMM-induced OA model was determined with ELISA after 8 weeks of DMM surgery (Figure 3.8A). The level of Col II IgG increased in the DMM-induced mouse model as compared to the normal healthy group. For the treatment, the nanoparticles were injected intradermally on the right side of the dorsal flank near the iLN. At week 8, Safranin O-Fast Green staining of the joints qualitatively showed that DMM surgery induced cartilage destruction and that LNP-Col II-R injection inhibited cartilage destruction more effectively than the other groups (Figure 3.8B). The osteoarthritis research society international (OARSI) score of the LNP-Col II-R group was significantly lower

than those of the other groups (Figure 3.8C). The size and maturity of osteophytes in the Safranin O-Fast Green staining images (Figure 3.8D) were quantified according to the scoring system (Figure 3.8E) [55, 56]. The LNP-R or LNP-Col II-R injection groups showed smaller size and lower maturity of osteophytes compared with other groups. The synovitis was analyzed by H&E staining of the joint synovium (Figure 3.8F). The synovial lining of the joints showed a higher extent of immune cell infiltration after DMM surgery in agreement with a previous study [57]. The LNP-Col II-R injection group showed lower degree of immune cell infiltration than the other groups. Terminal deoxynucleotidyl transferase dUTP nick end labeling (TUNEL) staining data at 8 weeks indicated that chondrocyte apoptosis was highly increased in all groups except for the LNP-Col II-R group as compared to the normal healthy group (Figure 3.8G). Col II in the cartilage was maintained at a higher level in the LNP-Col II-R-injected mice (Figure 3.8H and 3.8I). This is likely due to the decreased expression of matrix metalloproteinase 13 (MMP13) (Figure 3.8H and 3.8I), which degrades Col II, and the higher expression of Col II in the LNP-Col II-R-injected mice (Figure 3.8J). The lower level of Col II in the cartilage of the LNP group is likely due to the increased MMP13 expression and decreased Col II expression. At week 8, the animals' pain was evaluated by the mechanical allodynia test (von Frey test) and static weight-bearing test. The von Frey test measures the withdrawal force at which stimulation to the hind paw causes pain such that the animals withdraw their hind paw from the plate. The withdrawal force threshold of the LNP-Col II-R group was significantly higher than those of the other groups and similar to that of the normal healthy group (Figure 3.8K). The weight-bearing test showed that LNP-Col II-R injection more effectively relieved pain than injection of PBS, LNP or LNP-OVA-R (Figure 3.8L). Pain relief by LNP-Col II-R injection is likely due to

mitigated inflammation in the joint[58]. The normal group was used as the control in this study instead of the sham surgical group. Since the OARSI scores of the normal and sham surgical control groups were not different from each other (Figure 3.9), the lack of the sham surgical control would not affect the evaluation of the therapeutic efficacy.

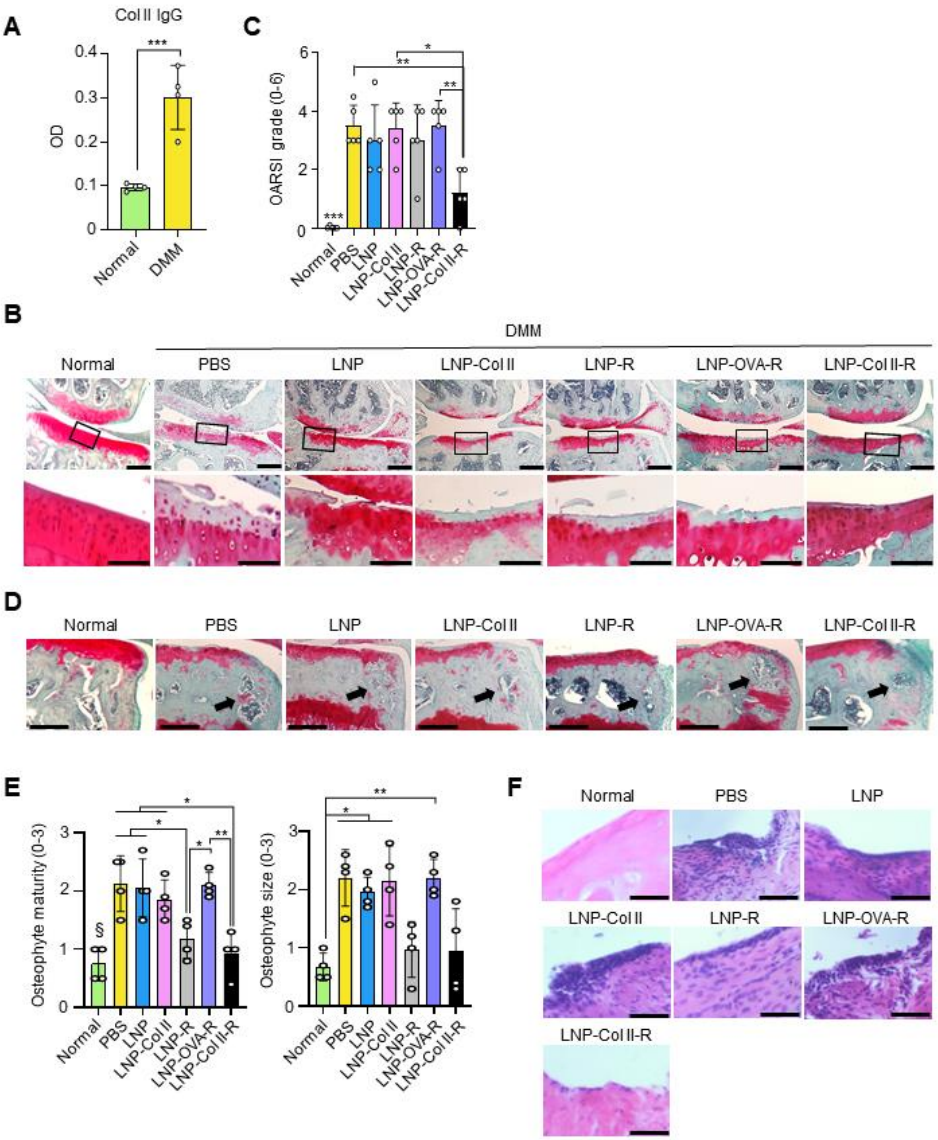
A
Col II IgG
OD
Normal
DMM
C
OARSI grade (0-6)
Normal
PBS
LNP
LNP-Col II
LNP-R
LNP-OVA-R
LNP-Col II-R
B
DMM
Normal
PBS
LNP
LNP-Col II
LNP-R
LNP-OVA-R
LNP-Col II-R
D
Normal
PBS
LNP
LNP-Col II
LNP-R
LNP-OVA-R
LNP-Col II-R
E
Osteophyte maturity (0-3)
Osteophyte size (0-3)
Normal
PBS
LNP
LNP-Col II
LNP-R
LNP-OVA-R
LNP-Col II-R
F
Normal
PBS
LNP
LNP-Col II
LNP-R
LNP-OVA-R
LNP-Col II-R

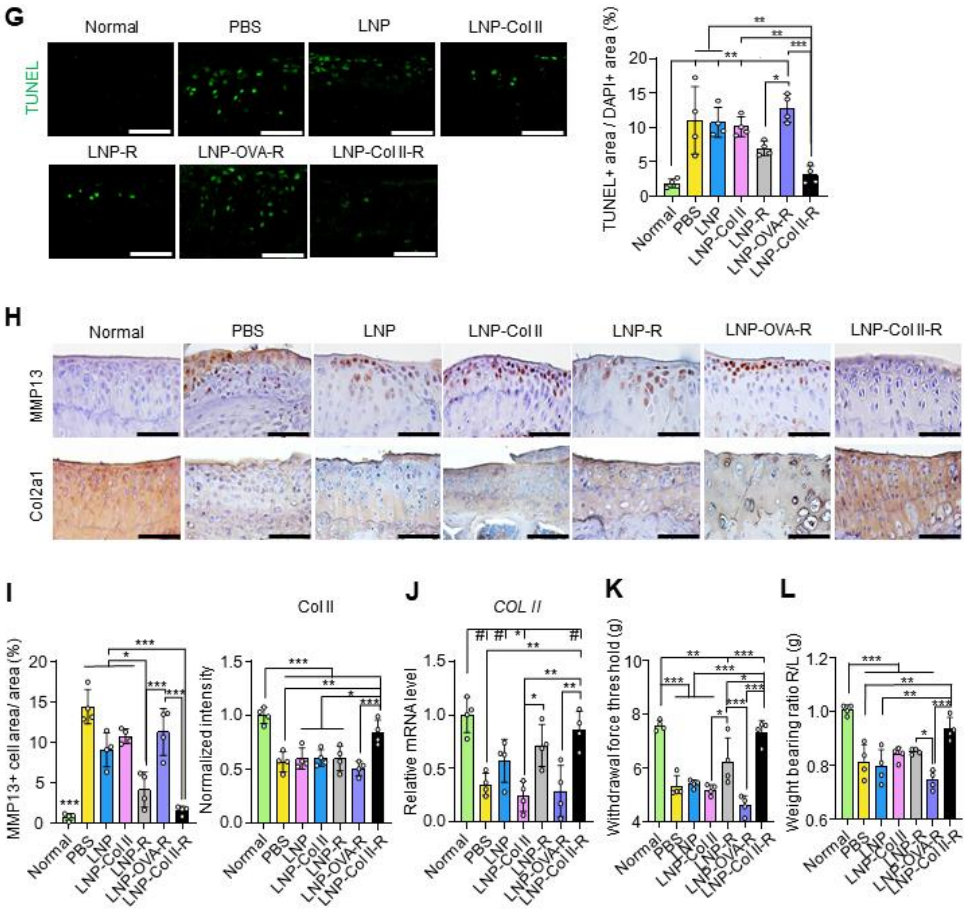

Figure 3.8. Therapeutic effects of LNP-Col II-R in OA mice at 8 weeks. (A) The level of autoantibodies against Col II in serum of DMM-induced mice. (n = 4). (B) Representative Safranin O-Fast Green-stained sections of the joints. Photographs of lower row are higher magnification of the rectangular areas of those in upper row. Scale bars = 100 μm. (C) Osteoarthritis research society international (OARSI) scores. *p<0.05, **p<0.01, ***p<0.001 versus any group except LNP-Col II-R. One way ANOVA with Tukey's post hoc test. (n = 5). (D) Representative Safranin O-Fast Green-stained sections of the joints. The osteophytes are indicated with black arrows. Scale bars = 100 μm, (E) Osteophyte

size and maturity analysis. *p<0.05, **p<0.01 , § p<0.001 versus any group except LNP-R and LNP-Col II-R. One way ANOVA with Tukey's post hoc test. (n = 4). (F) Hematoxylin and Eosin staining of the synovium. Scale bars = 100 µm. (G) Terminal deoxynucleotidyl transferase dUTP nick end labeling (TUNEL) staining of the cartilage. Scale bars = 100 µm. (H) Immunostaining for matrix metallopeptidase 13 (MMP13) and collagen type II alpha 1 chain (Col2a1) in the cartilage (Scale bars = 100µm) and (I) quantification. (J) Relative mRNA expressions Col II in the joints. (n = 4). Pain evaluated by (K) mechanical allodynia (von Frey) test and (L) static weight-bearing test. (A), (G), (I), (J), (K), and (L) *p<0.05, **p<0.01, ***p<0.001. One way ANOVA (multiple comparison) with Tukey's post hoc test. (n = 4).

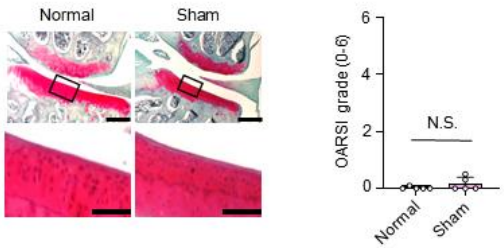

Figure 3.9. Comparison between sham surgical group and normal healthy group at 8 weeks. Shown are Safranin O-Fast Green staining result and OARSI scores. Photographs of lower row are higher magnification of the rectangular areas of those in upper row. N.S. : not significant. Two-tailed t test. Scale bars = 100 µm. (n = 5).

3.2.7. LNP-Col II-R mediated immune modulation in the synovium of OA mice

Inflammatory immune cells infiltrate the synovium of OA joint and are intimately involved in the progression of OA [4, 6, 8, 31, 45, 58, 59, 60, 61]. We investigated whether LNP-Col II-R injection could mitigate inflammation at the OA joint by modulating inflammatory immune cells in the synovium. Immunostaining analyses indicated that LNP-Col II-R injection significantly increased Tregs in the synovium at 8 weeks compared with the other treatments (Figure 3.10A). Meanwhile, immunostaining for a macrophage marker (F4/80) and an M1 macrophage marker (iNOS) indicated that LNP-Col II-R injection significantly reduced the number of inflammatory M1 macrophages in the synovium compared to the other treatments (Figure 3.10B). The number of anti-inflammatory M2 macrophages in the synovium was not significantly different among the LNP-Col II, LNP-R, and LNP-Col II-R groups (Figure 3.10C). Moreover, LNP-Col II-R injection reduced the densities of interferon-gamma (IFN-γ)-secreting CD4+ T cells, interleukin-17 (IL-17)-secreting CD4+ T cells and interleukin 1-beta (IL-1β)-secreting M1 macrophages in the synovium (Figure 3.10D, 3.10E and 3.10F). These results may be ascribed to the LNP-Col II-R injection-mediated increase in the number of anti-inflammatory IL-10-secreting Tregs in the synovium (Figure 3.10G) that inhibit inflammatory CD4+ T cells and M1 macrophages. PCR analyses showed tendencies for the expression of IFN-γ, IL-1β, TNF-α and TGF-β in the joints (Figure 3.10H), which were similar to the immunostaining results. LNP-Col II-R injection significantly decreased the mRNA expression of inflammatory cytokines (IFN-γ, IL-1β, and TNF-α) and increased that of the anti-inflammatory cytokine TGF-β in the OA joints.

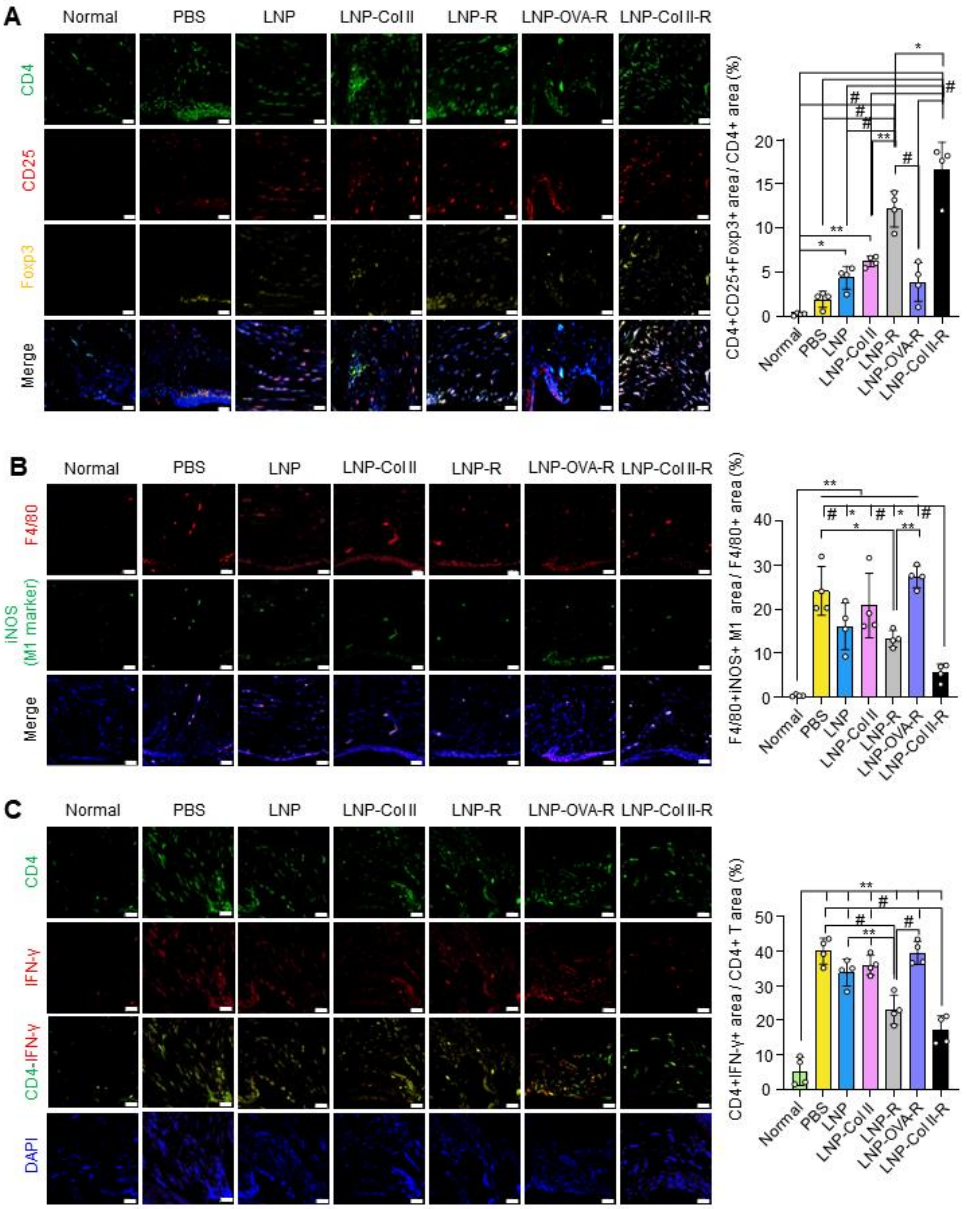
A
Normal
PBS
LNP
LNP-Col II
LNP-R
LNP-OVA-R
LNP-Col II-R
CD4
CD25
Foxp3
Merge
CD4+CD25+Foxp3+ area / CD4+ area (%)
B
F4/80
iNOS
(M1 marker)
F4/80+iNOS+ M1 area / F4/80+ area (%)
C
IFN-γ
CD4-IFN-γ
DAPI
CD4+IFN-γ+ area / CD4+ T area (%)

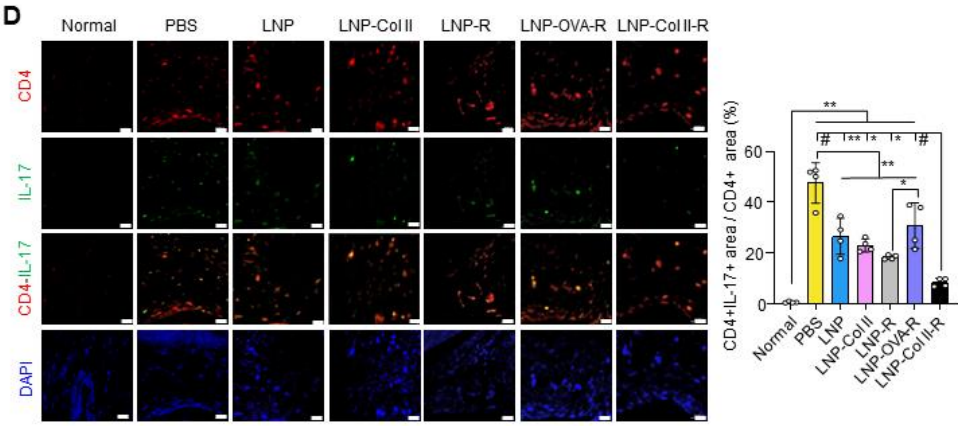
D
Normal
PBS
LNP
LNP-Col II
LNP-R
LNP-OVA-R
LNP-Col II-R
CD4
IL-17
CD4-IL-17
DAPI
CD4+IL-17+ area / CD4+ area (%)
Normal
PBS
LNP
LNP-Col II
LNP-R
LNP-OVA-R
LNP-Col II-R

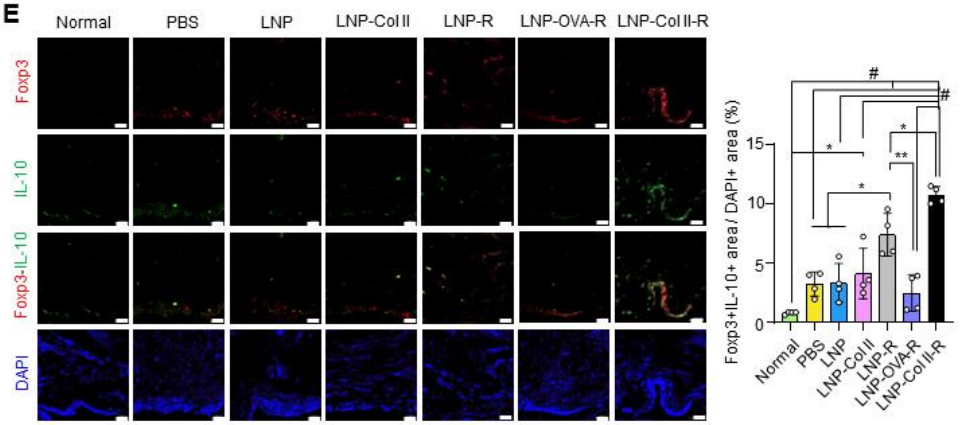
E
Normal
PBS
LNP
LNP-Col II
LNP-R
LNP-OVA-R
LNP-Col II-R
Foxp3
IL-10
Foxp3-IL-10
DAPI
Foxp3+IL-10+ area / DAPI+ area (%)
Normal
PBS
LNP
LNP-Col II
LNP-R
LNP-OVA-R
LNP-Col II-R

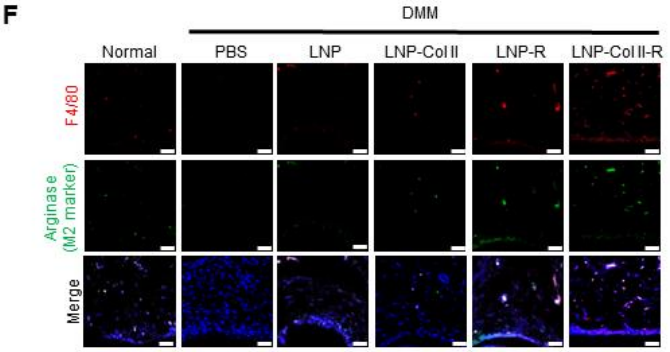
F
DMM
Normal
PBS
LNP
LNP-Col II
LNP-R
LNP-Col II-R
F4/80
Arginase
(M2 marker)
Merge

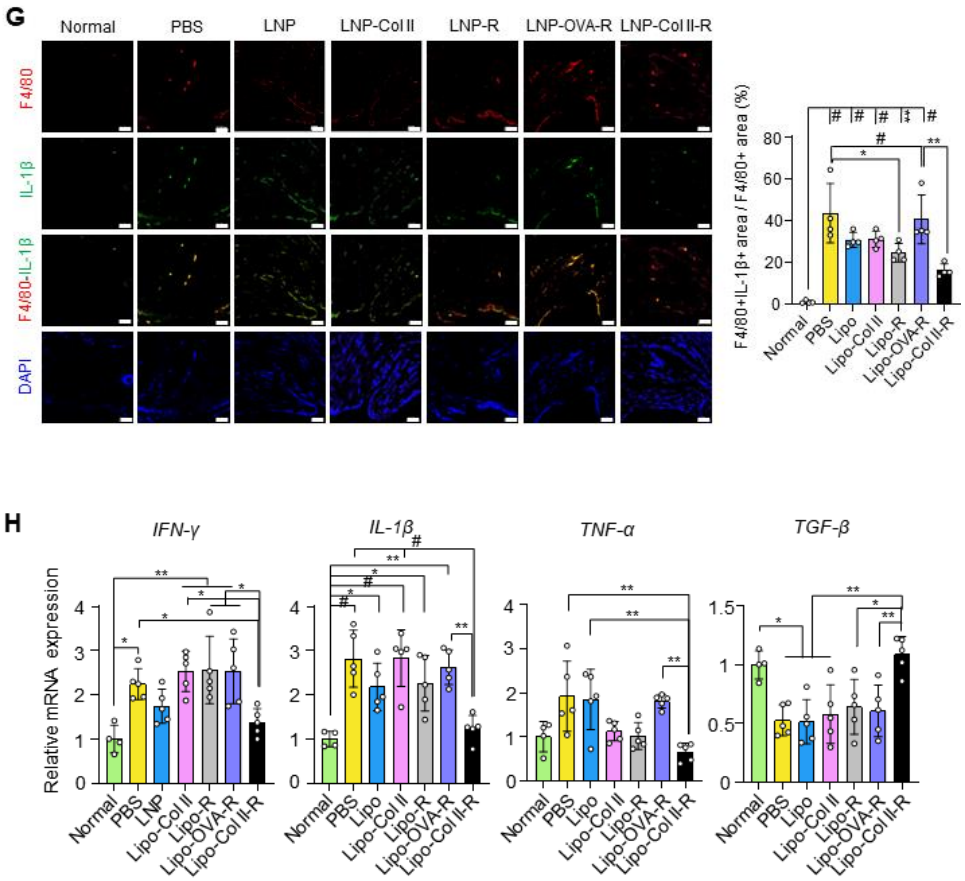

Figure 3.10. Immune modulation in the synovium of OA mice at 8 weeks. Immunostaining for (A) CD4+CD25+Foxp3+ Tregs, (B) F4/80+iNOS+ M1 macrophages, (C) CD4+IFN-γ+ T cells, (D) CD4+IL-17+ T cells, (E) Foxp3+IL-10+ Tregs, (F) F4/80+Arginase+ M2 macrophages, and (G) F4/80+IL-1β+ M1 macrophages in the synovium. (H) Relative mRNA expressions of IFN-γ, IL-1β, TNF-α and TGF-β in the joints. n = 5 except for the normal group (n = 4). (A-G) Scale bars = 20 μm. (n = 4). (A-H) *p<0.05, **p<0.01, #p<0.001. One way ANOVA (multiple comparison) with Tukey's post hoc test.

3.2.8. Therapeutic effects of adoptive cell transfer to OA mice

To investigate whether Tregs induced by LNP-Col II-R injection are responsible for the therapeutic effects, we performed adoptive T cell transfer to OA mice. CD4+CD25+ T cells that included Tregs were isolated from the spleens of mice that had been treated with intradermal injection of PBS, LNP-R, or LNP-Col II-R. The reason for sorting cells with only CD4 and CD25 without Foxp3 is to retain the cells' therapeutic effect. In order to isolate Foxp3+ Tregs, a cell permeabilizing step is necessary, which would kill the cells and make the cells unsuitable for the adoptive transfer [62]. In adoptive Treg transfer in clinical trials, therefore, CD4+CD25+CD127- or CD4+CD25+CD127-CD45RA+ T cells are sorted and transferred [40], while CD4+CD25+ T cells are sorted in murine model for adoptive Treg transfer [63]. The isolated CD4+CD25+ T cells were transferred to OA mice by intravenous injection (Figure 3.11A). Safranin O-Fast Green staining of the joints at 8 weeks indicated that the LNP-Col II-R group showed less destruction in the cartilage and scored significantly lower OARSI grades than the other groups (Figure 3.11B). Immunostaining analysis indicated that the number of CD4+CD25+Foxp3+ Tregs in the synovium was significantly higher in the LNP-Col II-R group than in the other groups (Figure 3.11C). These data suggest that Tregs induced by LNP-Col II-R injection are likely responsible for the therapeutic effects of LNP-Col II-R.

To determine whether CD11c+ DCs induced by LNP-Col II-R injection could alleviate OA, we performed adoptive DC transfer to OA mice. CD11c+ DCs were isolated from the right inguinal lymph nodes of mice that had been treated with intradermal injection of PBS, LNP-R, or LNP-Col II-R. The isolated CD11c+ cells were transferred to OA mice by intradermal injection. Safranin O-

Fast Green staining of the joints at 8 weeks indicated that the LNP-Col II-R group showed less destruction in the cartilage and significantly lower OARSI grade than the other groups (Figure 3.11D).

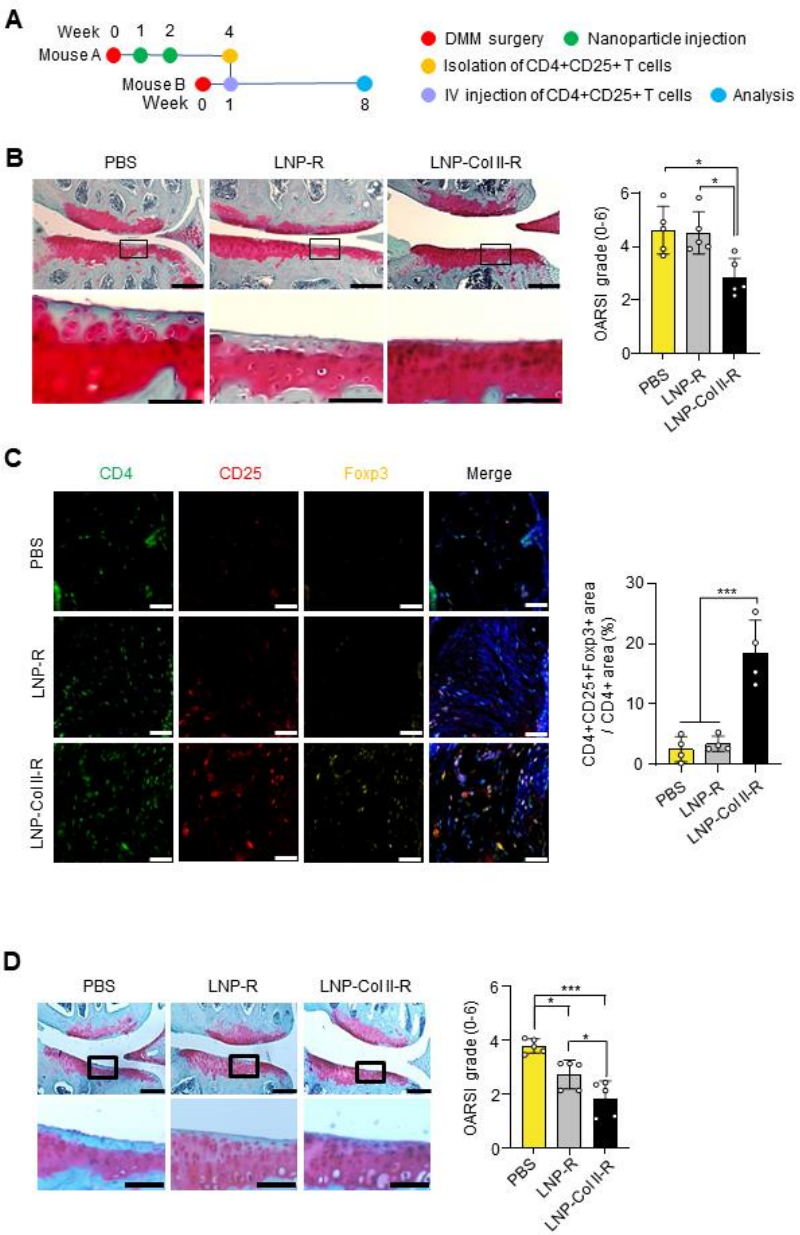

Figure 3.11. Therapeutic effects of adoptive cell transfer to OA mice. CD4+CD25+ T cells were isolated from mice treated with intradermal injection of PBS, LNP-R, or LNP-Col II-R. (A) Timeline of the experiment. (B) Representative Safranin O-Fast Green-stained sections of the cartilages and the OARSI grade 8 weeks after adoptive cell transfer. Photographs of lower row are higher magnification of the rectangular areas of those in upper row. Scale bars = 100 μm. (n = 5). (C) Immunostaining of Tregs in the synovium. Scale bars = 20 μm. (n = 4). CD11c+ DCs were isolated from mice treated with intradermal injection of PBS, LNP-R, or LNP-Col II-R. (D) Representative Safranin O-Fast Green-stained sections of the cartilages and the OARSI grade 8 weeks after adoptive cell transfer are shown. Photographs of lower row are higher magnification of the rectangular areas of those in upper row. Scale bars = 100 μm. (n = 5). (B), (C) and (D) *$p<0.05$, ***$p<0.001$. One way ANOVA (multiple comparison) with Tukey's post hoc test.

3.2.9. Toxicity of LNP-Col II-R

The cationic lipids are known to have destructive effects on cell membrane by forming pores or by disrupting cell membrane nonspecifically[64]. Toxicity increases with surface charge and size of nanoparticles[65, 66]. And toxicity of cationic nanoparticles could be compensated by PEG decoration on surface[67]. Considering that LNP-Col II-R nanoparticles have slightly positive charge with 6.2± 3.6 mV and decorated with PEG, the nanoparticles could have less destructive effect on cells. The cytotoxicity and in vivo organ toxicity of LNP-Col II-R were evaluated. DCs were treated with PBS, free Col II, or LNP-Col II-R in

vitro for 24 hours. The number of viable cells (Figure 3.12A) and the mRNA levels of apoptosis-related genes [Bcl-2-associated X protein (BAX) and Caspase-3] (Figure 3.12B) were not different among all the groups. Intradermal injection of LNP-Col II-R into mice did not exhibit toxicity to organs, as the blood serum levels of alanine aminotransferase (ALT), aspartate aminotransferase (AST), blood urea nitrogen (BUN) and creatinine were not changed by the injection (Figure 3.12C). Furthermore, histological examination of the major organs at 8 weeks showed no signs of organ damage or inflammation (Figure 3.12D). The results indicated that LNP-Col II-R did not cause cytotoxicity or organ toxicity.

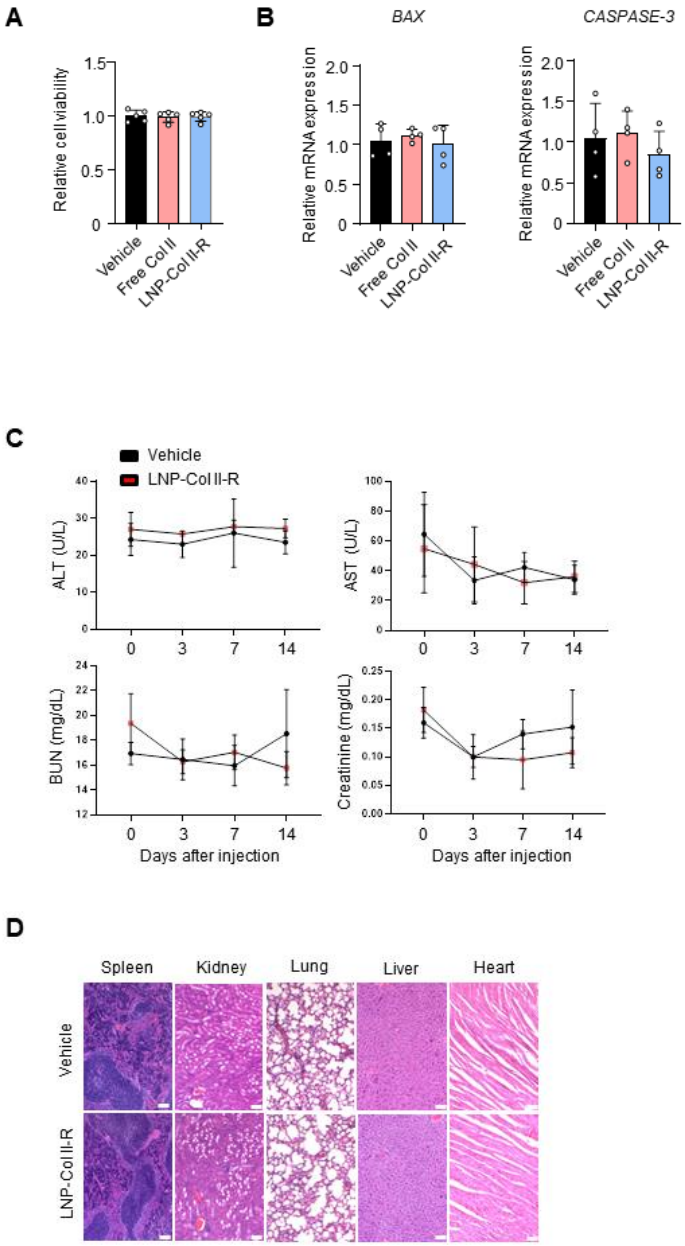

Figure 3.12. Toxicity of LNP-Col II-R. In vitro toxicity of LNP-Col II-R, as evaluated by (A) determining relative number of viable DCs in cultures after

various treatments and by (B) determining the expressions of apoptosis marker mRNAs in DCs in cultures after various treatments for 24 hours. No significant difference between any groups. (n = 4). (C) In vivo toxicity of LNP-Col II-R that was intradermally injected to OA mice, as evaluated by determining the blood levels of ALT, AST, BUN, and Creatinine. No significant difference between two groups. (n = 5). (D) In vivo organ toxicity of intradermally injected LNP-Col II-R, as evaluated by Hematoxylin and Eosin (H&E) staining of the major organs of OA mice at 8 weeks. Scale bars = 10 μm.

Chapter 4.

Conclusions and future studies

The OA pathology is heterogeneous and involves several factors, such as genetic, hormone- or age-related intrinsic factors and traumatic injury-induced extrinsic factors [1, 2]. Considering the heterogeneity of OA pathology, the proposed treatment may not be effective for OA as a whole and could specifically be effective for injury-induced inflammatory OA. Inflammatory immune cells, such as Th1 cells, Th17 cells, and M1 macrophages, in OA joints contribute to local inflammation, cartilage destruction, and pain. In OA progression, inflammatory immune cells secrete proinflammatory cytokines such as IL-1β, TNF-α, and IFN-γ, which induce chondrocyte apoptosis [68] and stimulate chondrocytes to produce cartilage matrix-degrading enzymes [e.g., MMP13 and a disintegrin and metalloproteinase 5 (ADAMTS5)] [69]. As OA progresses, the number of inflammatory immune cells, which infiltrate OA joints and secrete inflammatory cytokines and cartilage matrix-degrading enzymes, increases, which eventually increases damage to cartilage tissues and aggravates the disease. Additionally, inflammatory immune cells correlate with pain. Inflammatory immune cells, especially activated M1 macrophages and inflammatory T cells within the synovial membrane and fat pad beneath the patella, were increased in OA patients [70]. M1 macrophages are known to cause pain in OA by interacting with neurons [71]. The number of CD4+ T cells within the synovium has also been reported to be related to the pain level [70], implying that pain in OA is influenced by the overall inflammatory status within the joint. Th1 and Th17 cells intensify pain by secreting inflammatory cytokines and by stimulating inflammatory M1 macrophages, while Tregs weaken pain by secreting anti-inflammatory cytokines, especially IL-10 [72]. Col II-specific Tregs, which are generated by LNP-Col II-R injection, can migrate to inflammatory OA joints via chemotaxis and secrete anti-inflammatory cytokines such as IL-10 upon Treg activation via interaction with

Col II, a potential autoantigen in OA patients [32, 34, 35, 44, 45, 46], presented on MHC class II of antigen-presenting cells (e.g., activated B cells, DC, and macrophages) in OA synovium. The cytokines secreted from Tregs in OA joints can inhibit the inflammatory immune cells (Th1 cells, Th17 cells and M1 macrophages) in OA joints and mitigate the local inflammation, leading to pain relief and cartilage protection.

The LNP-Col II-R therapy inhibited cartilage destruction (Fig. 5B). This may result from both cartilage regeneration (Fig. 5J) and cartilage protection (Fig. 5G and 5H) induced by LNP-Col II-R. LNP-Col II-R protected cartilage from destruction by relieving inflammation (Fig. 6) and inhibiting MMP13 expression (Fig. 5H and 5I). A number of previous studies have demonstrated cartilage regeneration following resolution of inflammation in OA joints. A previous study demonstrated that removing senescent chondrocytes that secrete proinflammatory cytokines in OA joints in animal models induced cartilage regeneration [73]. In addition, intraarticular injection of mesenchymal stem cells, which exert anti-inflammatory paracrine action, into OA joints resulted in regeneration of the cartilage [74]. Inflammation resolution in joints inhibits the NF-κB signaling pathway in chondrogenic progenitor cells, which upregulates chondrogenesis [75]. Reduced levels of inflammatory cytokines recruit more progenitor cells around the site of the OA lesion for active chondrogenesis and decrease MMP13 expression [69], which would lead to increases in Col II expression and avoid Col II degradation in cartilage. Therefore, resolution of local inflammation in OA joint by LNP-Col II-R may lead to cartilage ECM protection and regeneration.

For clinical translation of LNP-Col II-R nanoparticle therapy, human peptide, DNA or mRNA of Col II or Col II epitope of MHC class II can be loaded

in LNPs. Meanwhile, this therapy may not be applied to all OA patients. Since OA pathology is heterogeneous and autoantibodies against Col II are found in approximately half of OA patients [45], this therapy could be applied to OA patients diagnosed with autoantibodies against Col II.

In summary, here we suggest tolerogenic nanoparticles that mitigate local inflammation in OA joints as an off-the-shelf treatment modality for OA. A previous study has demonstrated that intradermal injection of tolerogenic nanoparticles led to uptake of myocardial infarction-related antigen-laden nanoparticles by antigen presenting cells (APCs) in dermis, APC migration to adjacent lymph nodes and induction of Tregs that subsequently migrated to the infarction area [24]. Similarly, intradermal injection of LNP-Col II-R nanoparticles generated Col II-specific Tregs in vivo (Fig. 4C). A higher number of Col II-specific Tregs were observed in the joint of the LNP-Col II-R injection group compared to the other groups (Fig. 6A). CD4+CD25+ T cells isolated from spleen of LNP-Col II-R-injected mice and intravenously injected to DMM animals (adoptive Treg transfer) migrated to the diseased joints (Fig. 7C). These results suggest that intradermal injection of LNP-Col II-R leads to induction of antigen-specific Tregs that migrate to the target lesion to alleviate the disease. This therapy offers advantages over the current therapies for OA. NSAID treatments and intraarticular injection of hyaluronic acid focus on alleviating symptoms and offer only temporary therapeutic benefit.

Cell therapies for OA, such as autologous chondrocyte implantation and mesenchymal stem cell implantation, are invasive, costly, time-consuming, and complicated. In contrast, LNP-Col II-R nanoparticle therapy can not only relieve pain and prevent cartilage destruction, but is also simple, noninvasive, off-the-shelf, and cost-effective. Unlike adoptive transfer of polyclonal Tregs that has

potential side effects of non-specific systemic immune suppression, LNP-Col II-R nanoparticle therapy can avoid the side effects by inducing OA-specific immune tolerance.

Although the LNP-Col II-R nanoparticle therapy showed a therapeutic efficacy in the DMM animal model, the animal model has limitations. While the DMM surgical model is the gold standard in the field [1, 54], the model does not include all of the heterogeneous OA pathologies and is restricted to an initial inflammatory input driven by the surgical insult.

References

1. Manlapaz DG, Sole G, Jayakaran P, Chapple CM. Risk factors for falls in adults with knee osteoarthritis: a systematic review. *Pm&r* **11**, 745-757 (2019).

2. Henriksen M, Jørgensen LB, Aaboe J. Obesity and Walking: Implications for Knee Osteoarthritis and Plantar Heel Pain. *Curr. Obesity Reports* **1**, 160-165 (2012).

3. Driban JB, Sitler MR, Barbe MF, Balasubramanian E. Is osteoarthritis a heterogeneous disease that can be stratified into subsets? *Clin. Rheumatol.* **29**, 123-131 (2010).

4. Robinson WH*, et al.* Low-grade inflammation as a key mediator of the pathogenesis of osteoarthritis. *Nat. Rev. Rheumatol* .**12**, 580-592 (2016).

5. Pap T, Korb-Pap A. Cartilage damage in osteoarthritis and rheumatoid arthritis—two unequal siblings. *Nat. Rev. Rheumatol.* **11**, 606-615 (2015).

6. Li YS, Luo W, Zhu SA, Lei GH. T Cells in Osteoarthritis: Alterations and Beyond. *Front. Immunol.* **8**, 356 (2017).

7. Xie X*, et al.* Auto-antibodies to post-translationally modified proteins in osteoarthritis. *Osteoarthr. Cartil.* **29**, 924-933 (2021).

8. Haseeb A, Haqqi TM. Immunopathogenesis of osteoarthritis. *Clin.*

Immunol. **146**, 185-196 (2013).

9. De Lucia O*, et al.* Hyaluronic Acid Injections in the Treatment of Osteoarthritis Secondary to Primary Inflammatory Rheumatic Diseases: A Systematic Review and Qualitative Synthesis. *Adv. Ther.* **37**, 1347-1359 (2020).

10. Davies RL, Kuiper NJ. Regenerative medicine: a review of the evolution of autologous chondrocyte implantation (ACI) therapy. *Bioengineering* **6**, 22 (2019).

11. Musiał-Wysocka A, Kot M, Majka M. The pros and cons of mesenchymal stem cell-based therapies. *Cell Transplant.* **28**, 801-812 (2019).

12. Wang Y, Yi H, Song Y. The safety of MSC therapy over the past 15 years: a meta-analysis. *Stem cell Res. Ther.* **12**, 1-15 (2021).

13. Lombardo D, Kiselev MA. Methods of Liposomes Preparation: Formation and Control Factors of Versatile Nanocarriers for Biomedical and Nanomedicine Application. *Pharmaceutics* **14**, 543 (2022).

14. Allen TM, Cullis PR. Liposomal drug delivery systems: from concept to clinical applications. *Adv. Drug Deliv. Rev.* **65**, 36-48 (2013).

15. Birke H*, et al.* Chronic non-cancer pain and the epidemic prescription of opioids in the Danish population: trends from 2000 to 2013. *Acta Anaesthesiol. Scand.* **60**, 623-633 (2016).

16. Cao Y, Ma Y, Tao Y, Lin W, Wang P. Intra-articular drug delivery for osteoarthritis treatment. *Pharmaceutics* **13**, 2166 (2021).

17. Zhang S, Gao H, Bao G. Physical principles of nanoparticle cellular endocytosis. *ACS nano* **9**, 8655-8671 (2015).

18. FOGED C, ARIGITA C, SUNDBLAD A, JISKOOT W, STORM G, FROKJAER S. Interaction of dendritic cells with antigen-containing liposomes: effect of bilayer composition. *Vaccine* **22**, 1903-1913 (2004).

19. Abdul Ghaffar K, Kumar Giddam A, Zaman M, Skwarczynski M, Toth I. Liposomes as nanovaccine delivery systems. *Curr. Top. Med. Chem.* **14**, 1194-1208 (2014).

20. Copland MJ*, et al.* Liposomal delivery of antigen to human dendritic cells. *Vaccine* **21**, 883-890 (2003).

21. Loeser RF*, et al.* Microarray analysis reveals age-related differences in gene expression during the development of osteoarthritis in mice. *Arthritis Rheumatol.* **64**, 705-717 (2012).

22. Van der Kraan P. Factors that influence outcome in experimental osteoarthritis. *Osteoarthr. Cartil.* **25**, 369-375 (2017).

23. Ma H-L, Blanchet T, Peluso D, Hopkins B, Morris E, Glasson S. Osteoarthritis severity is sex dependent in a surgical mouse model. *Osteoarthr. Cartil.* **15**, 695-700 (2007).

24. Kwon SP*, et al.* Nanoparticle-Mediated Blocking of Excessive Inflammation for Prevention of Heart Failure Following Myocardial Infarction. *Small* **17**, 2101207 (2021).

25. Malissen B, Tamoutounour S, Henri S. The origins and functions of dendritic cells and macrophages in the skin. *Nat. Rev. Immunol.* **14**, 417-428 (2014).

26. Hu J*, et al.* Loganin ameliorates cartilage degeneration and osteoarthritis development in an osteoarthritis mouse model through inhibition of NF-κB activity and pyroptosis in chondrocytes. *J. Ethnopharmacol.* **247**, 112261 (2020).

27. Kim J-H*, et al.* Matrix cross-linking–mediated mechanotransduction promotes posttraumatic osteoarthritis. *Proc Natl Acad Sci U S A* **112**, 9424-9429 (2015).

28. Kim H, Lee B-K. Anti-inflammatory effect of adipose-derived stromal vascular fraction on osteoarthritic temporomandibular joint synoviocytes. *Tissue. Eng. Regen. Med.* **17**, 351-362 (2020).

29. Wood MJ*, et al.* Macrophage proliferation distinguishes 2 subgroups of knee osteoarthritis patients. *JCI Insight* **4**, e125325 (2019).

30. Benito MJ, Veale DJ, FitzGerald O, Van Den Berg WB, Bresnihan B. Synovial tissue inflammation in early and late osteoarthritis. *Ann. Rheum. Dis.* **64**, 1263-1267 (2005).

31. Moradi B*, et al.* CD4+ CD25+/high CD127 low/-regulatory T cells are enriched in rheumatoid arthritis and osteoarthritis joints—analysis of frequency and phenotype in synovial membrane, synovial fluid and peripheral blood. *Arthritis Res. Ther.* **16**, 1-13 (2014).

32. Yuan GH, Masuko-Hongo K, Kato T, Nishioka K. Immunologic intervention in the pathogenesis of osteoarthritis. *Arthritis Rheum.* **48**, 602-611 (2003).

33. Lopes EBP, Filiberti A, Husain SA, Humphrey MB. Immune Contributions to Osteoarthritis. *Curr. Osteoporos. Rep.* **15**, 593-600 (2017).

34. Sakata M*, et al.* Osteoarthritic articular chondrocytes stimulate autologous T cell responses in vitro. *Clin. Exp. Rheumatol.* **21**, 704-710 (2003).

35. Da RR, Qin Y, Baeten D, Zhang Y. B cell clonal expansion and somatic hypermutation of Ig variable heavy chain genes in the synovial membrane of patients with osteoarthritis. *J. Immunol.* **178**, 557-565 (2007).

36. Du H*, et al.* The prevalence of autoantibodies against cartilage intermediate layer protein, YKL-39, osteopontin, and cyclic citrullinated peptide in patients with early-stage knee osteoarthritis: evidence of a variety of autoimmune processes. *Rheumatol. Int.* **26**, 35-41 (2005).

37. Tiemessen MM, Jagger AL, Evans HG, van Herwijnen MJ, John S, Taams LS. CD4+ CD25+ Foxp3+ regulatory T cells induce alternative activation of human monocytes/macrophages. *Proc Natl Acad Sci U S*

A **104**, 19446-19451 (2007).

38. Coombes JL, Robinson NJ, Maloy KJ, Uhlig HH, Powrie F. Regulatory T cells and intestinal homeostasis. *Immunol. rev.* **204**, 184-194 (2005).

39. Duffy SS, Keating BA, Moalem-Taylor G. Adoptive transfer of regulatory T cells as a promising immunotherapy for the treatment of multiple sclerosis. *Front. Neurosci.* **13**, 1107 (2019).

40. Romano M, Fanelli G, Albany CJ, Giganti G, Lombardi G. Past, present, and future of regulatory T cell therapy in transplantation and autoimmunity. *Front. Immunol.* **10**, 43 (2019).

41. Kim YC*, et al.* Engineered antigen-specific human regulatory T cells: immunosuppression of FVIII-specific T-and B-cell responses. *Am. J. Hematol.* **125**, 1107-1115 (2015).

42. Tarbell KV, Yamazaki S, Olson K, Toy P, Steinman RM. CD25+ CD4+ T cells, expanded with dendritic cells presenting a single autoantigenic peptide, suppress autoimmune diabetes. *Journal of Experimental Medicine* **199**, 1467-1477 (2004).

43. Wang M*, et al.* MMP13 is a critical target gene during the progression of osteoarthritis. *Arthritis Res. Ther.* **15**, 1-11 (2013).

44. Takagi T, Jasin HE. Interactions between anticollagen antibodies and chondrocytes. *Arthritis & Rheumatism: Official Journal of the American College of Rheumatology* **35**, 224-230 (1992).

45. Sakkas LI, Platsoucas CD. The role of T cells in the pathogenesis of osteoarthritis. *Arthritis. Rheum.* **56**, 409-424 (2007).

46. Lohmander LS, Atley LM, Pietka TA, Eyre DR. The release of crosslinked peptides from type II collagen into human synovial fluid is increased soon after joint injury and in osteoarthritis. *Arthritis. Rheum.* **48**, 3130-3139 (2003).

47. Eloy JO*, et al.* Co-loaded paclitaxel/rapamycin liposomes: Development, characterization and in vitro and in vivo evaluation for breast cancer therapy. *Colloids Surf B Biointerfaces* **141**, 74-82 (2016).

48. Stoll S. Dynamic Imaging of T Cell-Dendritic Cell Interactions in Lymph Nodes. *Science* **296**, 1873-1876 (2002).

49. Huh JC*, et al.* Bidirectional interactions between antigen-bearing respiratory tract dendritic cells (DCs) and T cells precede the late phase reaction in experimental asthma: DC activation occurs in the airway mucosa but not in the lung parenchyma. *The Journal of experimental medicine* **198**, 19-30 (2003).

50. Mundra V, Mahato RI. Design of nanocarriers for efficient cellular uptake and endosomal release of small molecule and nucleic acid drugs: learning from virus. *Front. Chem. Sci. Eng.* **8**, 387-404 (2014).

51. Rayamajhi S, Marchitto J, Nguyen TDT, Marasini R, Celia C, Aryal S. pH-responsive cationic liposome for endosomal escape mediated drug delivery. *Colloids and Surfaces B: Biointerfaces* **188**, 110804 (2020).

52. Fischer R, Turnquist HR, Taner T, Thomson AW. Use of rapamycin in the induction of tolerogenic dendritic cells. *Dendritic Cells*, 215-232 (2009).

53. Snir O*, et al.* Multifunctional T cell reactivity with native and glycosylated type II collagen in rheumatoid arthritis. *Arthritis Rheum.* **64**, 2482-2488 (2012).

54. Glasson SS, Blanchet TJ, Morris EA. The surgical destabilization of the medial meniscus (DMM) model of osteoarthritis in the 129/SvEv mouse. *Osteoarthr. Cartil.* **15**, 1061-1069 (2007).

55. Little C*, et al.* Matrix metalloproteinase 13–deficient mice are resistant to osteoarthritic cartilage erosion but not chondrocyte hypertrophy or osteophyte development. *Arthritis Rheum.* **60**, 3723-3733 (2009).

56. Glasson S, Chambers M, Van Den Berg W, Little C. The OARSI histopathology initiative–recommendations for histological assessments of osteoarthritis in the mouse. *Osteoarthr. Cartil.* **18**, S17-S23 (2010).

57. Wu CL*, et al.* Conditional macrophage depletion increases inflammation and does not inhibit the development of osteoarthritis in obese macrophage Fas-induced apoptosis–transgenic mice. *Arthritis Rheum.* **69**, 1772-1783 (2017).

58. Bonnet CS, Walsh DA. Osteoarthritis, angiogenesis and inflammation. *Rheum.* **44**, 7-16 (2005).

59. Berenbaum F. Osteoarthritis as an inflammatory disease (osteoarthritis

is not osteoarthrosis!). *Osteoarthr. Cartil.* **21**, 16-21 (2013).

60. de Lange-Brokaar BJ*, et al.* Synovial inflammation, immune cells and their cytokines in osteoarthritis: a review. *Osteoarthr. Cartil.* **20**, 1484-1499 (2012).

61. Mathiessen A, Conaghan PG. Synovitis in osteoarthritis: current understanding with therapeutic implications. *Arthritis. Res. Ther.* **19**, 18 (2017).

62. Singer BD, King LS, D'Alessio FR. Regulatory T cells as immunotherapy. *Front. Immunol.* **5**, 46 (2014).

63. Xu W*, et al.* Adoptive transfer of induced-Treg cells effectively attenuates murine airway allergic inflammation. *PloS one* **7**, e40314 (2012).

64. Takahashi H, Caputo GA, Vemparala S, Kuroda K. Synthetic random copolymers as a molecular platform to mimic host-defense antimicrobial peptides. *Bioconjug. Chem.* **28**, 1340-1350 (2017).

65. Weiss M*, et al.* Density of surface charge is a more predictive factor of the toxicity of cationic carbon nanoparticles than zeta potential. *J. nanobiotechnology* **19**, 1-19 (2021).

66. Wei X*, et al.* Cationic nanocarriers induce cell necrosis through impairment of Na+/K+-ATPase and cause subsequent inflammatory response. *Cell research* **25**, 237-253 (2015).

67. Lv H, Zhang S, Wang B, Cui S, Yan J. Toxicity of cationic lipids and cationic polymers in gene delivery. *J. control. release* **114**, 100-109 (2006).

68. Aizawa T, Kon T, Einhorn T, Gerstenfeld L. Induction of apoptosis in chondrocytes by tumor necrosis factor-alpha. *J. Orthop. Res.* **19**, 785-796 (2001).

69. Hu Q, Ecker M. Overview of MMP-13 as a Promising Target for the Treatment of Osteoarthritis. *Int. J. Mol. Sci.* **22**, 1742 (2021).

70. Greif DN*, et al.* Infrapatellar fat pad/synovium complex in early-stage knee osteoarthritis: potential new target and source of therapeutic mesenchymal stem/stromal cells. *Front. Bioeng. Biotechnol.* **8**, 1-16 (2020).

71. Geraghty T, Winter DR, Miller RJ, Miller RE, Malfait A-M. Neuroimmune interactions and osteoarthritis pain: focus on macrophages. *Pain Reports* **6**, e892 (2021).

72. Kavelaars A, Heijnen CJ. T Cells as Guardians of Pain Resolution. *Trends Mol. Med.* **27,** 302-313 (2021).

73. Jeon OH*, et al.* Local clearance of senescent cells attenuates the development of post-traumatic osteoarthritis and creates a pro-regenerative environment. *Nat. Med.* **23**, 775-781 (2017).

74. Park YB, Ha CW, Lee CH, Yoon YC, Park YG. Cartilage regeneration in

osteoarthritic patients by a composite of allogeneic umbilical cord blood-derived mesenchymal stem cells and hyaluronate hydrogel: results from a clinical trial for safety and proof-of-concept with 7 years of extended follow-up. *Stem Cells Transl. Med.* **6**, 613-621 (2017).

75. Li M, Xiao R, Li J, Zhu Q. Regenerative approaches for cartilage repair in the treatment of osteoarthritis. *Osteoarth. Cartil.* **25**, 1577-1587 (2017).

요약 (국문초록)

골관절염(osteoarthritis)은 류머티즘 관절염과 함께 가장 대표적인 관절질환으로 알려져 있다. 골관절염은 병증진행과 함께 관절 주변 골의 과잉 형성, 관절 변형과 통증 및 점진적 운동 장애를 동반한다. 현재 전 세계 55세 이상 인구의 약 80%와 75세 이상 고령 인구의 거의 대부분이 퇴행성관절염 소견을 보이는 것으로 알려져 있다. 우리나라의 경우, 사회의 고령화가 급속도로 진행됨에 따라 골관절염으로 인한 통증을 호소하는 인구가 점차 증가하고 있으며, 노령인구에서뿐 아니라 젊은 인구 층에서도 환경적, 유전적 요인으로 인해 골관절염 발생이 증가하면서 골관절염으로 인한 의료비 지출 역시 빠른 속도로 증가하고 있는 추세이다.

현재까지 알려진 골관절염 치료방법으로는 항 염증성 약물투여, 생활 및 식습관을 개선하는 비약물요법 그리고 침습적 방법으로 관절을 수술하는 외래적 치료방법이 있다. 비스테로이드성 항염증 약물의 경우, 염증완화를 통한 통증 감소에는 효과적이나 위장관 부작용이 발생할 수 있고, 이 대안으로 사용된 약물인 COX-2 저해제의 경우는 심혈관계 부작용 및 위장관 손상을 일으킬 수 있다. 또한 외래적 수술방법의 경우, 효과적으로 통증의 원인을 제거할 수 있으나, 관절의 상태와 인공관절의 상태에 따라 재수술 가능성의 부담이

존재한다.

대개, 골관절염은 물리적 요인이 원인인 것으로 알려져 있으나, 최근 다수 논문들을 통해 골관절염에 면역체계가 관여하는 것이 알려지면서, 골관절염에서의 면역세포 작용의 이해 및 이를 바탕으로 한 면역조절이 중요성을 갖게 되었다.

본 연구에서는 제 2형 콜라겐 펩타이드 및 라파마이신을 담지하는 면역조절 나노입자를 골관절염 치료에 적용하였다. 실험 결과, 제 2형 콜라겐 펩타이드 및 라파마이신을 담지한 나노입자는 관용 수지상 세포를 유도시키고, 더 나아가 항원특이적 항염증성 조절 T 세포를 유도시켰다. 또한 관절에서 발생하는 염증성 면역세포에 의한 염증반응을 감소시키면서, 염증반응으로 수반되는 연골 파괴 및 통증을 완화시켰다. 주조직적합성 복합체 클래스 II에 항원을 제시하는 관용 수지상 세포 및 항원특이적 조절 T 세포가 골관절염 치료효과를 갖는지 여부를 확인하지 위해 각 세포를 이용한 입양전달 실험을 추가적으로 실시하였고, 그 결과 추가적인 나노입자의 주입 없이도 골관절염이 완화되는 것을 확인하였다.

종합하여, 우리는 제 2형 콜라겐 펩타이드 및 라파마이신을 담지한 면역조절 나노입자가 골관절염에 치료효능을 갖는 것을 확인하였다. 본 실험에서 사용된 나노입자는 더 나아가 골관절염뿐 아니라, 제 2형 콜라겐 펩타이드 대신 다른 질병 항원을 담지 시키면 심근경색,

뇌경색, 척추손상 등의 염증성 질환 또는 아토피, 류마티스관절염, 1형 당뇨병, 크론병, 루푸스 등 자가면역질환의 치료제로서도 활용할 수 있다.

주요어: 관용 지질 나노입자, 관용 수지상세포, 대식세포, 조절 T세포, 면역조절, 골관절염, 활막염

학번: 2017-20762